Bioenergetic Evaluation of Site-specific Keloid and FKN Fibroblasts

By Temwani Chalwa

(CHLTEM001)

SUBMITTED TO THE UNIVERSITY OF CAPE TOWN

In fulfilment of the requirements for the degree

MScMed in Trichology and Cosmetic Science

Division of Dermatology

Faculty of Health Sciences

University of Cape Town

July 2019

Supervisor: Prof Nonhlanhla Khumalo

Co-supervisor: Prof Ardeshir Bayat

Co-supervisor: Dr Maribanyana Lebeko

University of Cape Town

The copyright of this thesis vests in the author. No quotation from it or information derived from it is to be published without full acknowledgement of the source. The thesis is to be used for private study or non-commercial research purposes only.

Published by the University of Cape Town (UCT) in terms of the non-exclusive license granted to UCT by the author.

University of Cape Town

The copyright of this thesis vests in the author. No quotation from it or information derived from it is to be published without full acknowledgement of the source. The thesis is to be used for private study or non-commercial research purposes only.

Published by the University of Cape Town (UCT) in terms of the non-exclusive license granted to UCT by the author.

DECLARATION

I, Temwani Chalwa, hereby declare that the work on which this dissertation/thesis is based is my original work (except where acknowledgements indicate otherwise) and that neither the whole work nor any part of it has been, is being, or is to be submitted for another degree in this or any other university.

I empower the university to reproduce for the purpose of research either the whole or any portion of the contents in any manner whatsoever.

Signed by candidate

Temwani Chalwa

July 2019

ACKNOWLEDGEMENTS

Firstly, I would like to thank the man upstairs "All things work together for good"

I'd like to thank my funders the National Research foundation for their support in making this study possible for me.

To my supervisors I can't thank you enough for the opportunity, guidance and support during this project. This has given me so much growth and made me a much better scientist. Prof Khumalo thank you for having me be member of the amazing HSR Lab; You truly have created something special here. Your lessons on work ethic will also never be forgotten. Prof Bayat thank you for your experience and expertise that was invaluable in the formulation of the research topic and the methodology. Dr. Lebeko, as much as I thank you for your guidance especially with all the tissue culture work and project plans, the thing I would like to thank you for the most is your truly caring about my personal wellbeing. I will forever appreciate your open-door policy and the times you would squat at my desk just to check in to see how I was doing. That meant so much to me and for that I will forever be grateful.

To my colleagues at the HSR lab, you guys are great! Thank you all for being who you are and making my time in the lab more interesting and pleasurable! Would really not have made it through this period without this eclectic bunch of people. The healthy banter made for great interjections between the hard work and late nights.

To my family, thank you all for your love and support in your individual ways. I'll forever be grateful for being lucky enough to have such a loving family in my life. Thanks to all my friends for getting me through this period. I appreciate you guys a lot and have probably thanked you already countless times for your support, and if you need me to name you in my thesis to know that then you're really not my true friend.

TABLE OF CONTENTS

LIST OF TABLES AND FIGURES

ABBREVIATIONS

µg/ml micrograms per millilitre

2-DG 2-deoxyglucose

AKN Acne Keloidalis Nuchae

ADP adenosine diphosphate

ATP adenosine triphosphate

AKR1C3 Aldo-keto reductase 1C3

AA arachidonic acid

bFGF basic fibroblast growth factor

BSA bovine serum albumin

CI cell index

CoA coenzyme A

Cyt C cytochrome C

ddH2O double distilled water

DAG diacylglycerol

DMEM Dulbecco's Modified Eagle's medium

DNA dioxyribonucleic acid

DOPA dihydroxyphenylalanine

ECAR extracellular acidification rate

ECL enhanced chemiluminescence

ECM Extracellular matrix

EDTA ethylenediaminetetraacetic acid

EGF epidermal growth factor

EGFR epidermal growth factor receptor

EPA eicosapentaenoic acid

ETC Electron Transport Chain

$FADH_2$ Flavin adenine dinucleotide

FAP-1α fibroblast activation protein 1α

FBS foetal bovine serum

Fb Fibroblasts

FCCP Carbonyl cyanide-4 (trifluoromethoxy) phenylhydrazone

FDG-PET fluorine-18-fluorodeoxyglucose positron emission tomography

FKN Folliculitis Keloidalis Nuchae

HCl hydrochloric acid

IGF-1 insulin-like growth factor 1

IL-1 interleukin-1

KI Intralesional Keloid Fibroblasts

KP Perilesional Keloid Fibroblasts

kDa kilo Dalton

MMPs matrix metalloproteinases

mg/ml milligram per millilitre

ml millilitre

mM millimolar

NADH nicotinamide adenine dinucleotide

NADPH Nicotinamide adenine dinucleotide phosphate

NS normal skin primary human fibroblasts

NSc normal scar primary human fibroblasts

NRG1 neuregulin-1

OXPHOS Oxidative phosphorylation

O_2/CO_2 oxygen/carbon dioxide

OCR oxygen consumption rate

PBS phosphate buffered saline

PDGF platelet-derived growth factor

PDGF platelet derived growth factor

PDL Pulsed dye laser

Pen/Strep Penicillin/streptomycin

PDG2 Prostaglandin D2

qs quantity sufficient

RIPA radio-immunoprecipitation assay

ROS reactive oxygen species

RTCA real time cell analysis

rpm revolutions per minute

SDS-PAGE sodium dodecyl sulphate polyacrylamide gel electrophoresis

SMAD mothers against decapentaplegic

SNPs single nucleotide polymorphisms

TBS-T tris-buffered saline and tween 20

TE trypsin-EDTA

TGF transforming growth factor

TGF-ß transforming growth factor beta

TNFα tumour necrosis factor alpha

VEGFA vascular endothelial growth factor A

ABSTRACT

Excessive scarring due to fibrosis from aberrant wound healing can lead to conditions such as Keloids or Folliculitis Keloidalis Nuchae (FKN). These fibroproliferative growths pose therapeutic challenges due to their complex aetiology that has been linked to multiple genetic and environmental factors, with frequent reoccurrence following therapy. Owing to reports on an increase in ATP and Fibroblast Activation Protein-1α production in keloids, the aim of this study was to investigate whether the disease phenotypes were linked to bioenergetic changes at a cellular level in these two conditions.

Patient-derived tissue biopsies were used for fibroblast cell culture models, in which cell analysis was carried out to assess phenotype and different parameters of bioenergetic cellular behaviour. In addition to FKN and the intra- and peri-lesional Keloid patient fibroblasts, normal skin and non-hypertrophic (normo-trophic) scar fibroblasts were used as negative controls.

The results show statistically significant and variable growth dynamics with increased proliferation and migration in keloid fibroblasts, while FKN fibroblasts showed a statistically significant increase in proliferation but had a similar migration profile to controls. The results further show that there is a statistically significant metabolic switch towards aerobic glycolysis in the fibroblasts from the disease conditions. During functional measurement of mitochondrial parameters, an increase in oxidative phosphorylation was exhibited in the disease conditions indicating their mitochondria were still functional. An increase in basal glycolysis with a concomitant increase in the cellular maximum glycolytic capacity was also demonstrated. Furthermore, protein analysis showed an upregulation in the expression of Fibroblast Activation Protein-1α in fibroblasts from both disease conditions.

This study begins to give novel insight into the bioenergetics of normal scars and scarring conditions such as FKN and, adds to the knowledge on the heterogeneity of fibroblasts derived from specific lesional sites within Keloids. These findings suggest that Keloids and FKN have a switch to a metabolic phenotype of aerobic glycolysis. This increase in glycolytic flux potentially proposes glycolytic inhibitors as a mechanistic basis for the treatment of these conditions.

CHAPTER 1. LITERATURE REVIEW

1.1. Introduction

Pathological scarring of a fibrotic nature has been shown to be one of the most challenging types of lesions for dermatologists and plastic surgeons to treat successfully. In addition to the multiple genetic factors at play, environmental factors have also been linked to the condition. It has also been suggested that increased skin pigmentation may play a role as these conditions are more prevalent in people of African ancestry[1].

Pathological scarring occurs when the normal wound healing response gets derailed and this may lead to the formation of scarring diseases like Keloids or Folliculitis Keloidalis Nuchae (FKN). This occurs when the delicate balance between the production and deposition of collagen as well as other extracellular matrix (ECM) components and the degradation of these components gets perturbed. This imbalance results in accumulation of tissue biomass giving rise to the irregular, progressive, exophytic scar lesions, which are often symptomatically painful and tender[2].

Keloids are benign fibroproliferative cutaneous growths that occur post wounding or trauma to the skin which includes piercings, surgery and thermal or chemical burns[3]. Unique to humans, familial inheritance is strong, and their occurrence is higher in individuals of African, Hispanic and Asian descent. These aggressive scars invade surrounding tissue and are irreversible. They exhibit extremely high rates of recurrence and unsatisfactory clinical management[4]. Many therapies for this condition are currently being used in clinical practice including surgical excision, steroid injections, laser and radiation. However, none of them have proved to be completely successful. The lack of a validated animal model for this disease has also augmented the failure to find a satisfactory treatment[5].

FKN, which is often incorrectly referred to as acne keloidalis (AKN), on the other hand is a fibrotic condition that is usually localised to the nuchal region of the scalp and features chronic inflammation of the hair follicles with papule formation. The initially formed papules with exiting hair then tend to merge to form prominent firm keloid like nodules and plaques eventually leading to scarring alopecia[6]. Some of the therapies that have been used for the treatment of this disease include antibiotics such as tetracyclines, surgical excision, steroid injections and laser. The exact aetiology is still unknown, due to very little research being carried out on the condition.

Apart from the adverse psychosocial effects these disfiguring scars cause[7], some patients may also experience contractures, pain and pruritus making the need for treatment not only purely for cosmetic purposes[8].

Metabolism is fast becoming an area of focus in research on fibrotic conditions as well as in cancers. In conditions such as lung fibrosis, defective fatty acid metabolism has recently been shown to promote the disease[9]. Defective metabolism has also been shown to be a factor in the pathogenesis of kidney fibrosis[10]. Moreover, a reprogramming of energetic metabolism has been reported in Alzheimer's disease and further perturbations to metabolism have been linked to other conditions[11,12].

In cancer, numerous studies have noted a reprogramming of the metabolism of cancer cells as tumorigenesis is dependent on it. A hallmark of the metabolism of cancer cells is the capacity to obtain and utilize nutrients needed for the maintenance of the cell's viability as well as increasing the biomass. This is often in nutrient deficient conditions and leads to changes in the cellular differentiation and tumour microenvironment. Known cancer-associated metabolic reprogramming includes the use of the glycolysis/Krebs cycle often exhibiting the well-defined Warburg effect of aerobic glycolysis. The glycolysis/Krebs cycle intermediates are utilized for biosynthesis as well as NADPH production. In addition to changes in the uptake of glucose and amino acids as well as changes in the metabolic interaction with the tumour microenvironment, gene regulation is also altered[13–15].

Owing to the work on metabolism in cancers and the other fibrotic conditions, as well as the similarities that keloids and FKN hold to neoplastic lesions, particular interest in this project lays on looking at the metabolism of keloid and FKN fibroblasts in comparison to normal skin and normal scar fibroblasts. This would help elucidate the status of metabolism and role that metabolic reprogramming has in these disease conditions. In so doing this will add to the body of knowledge and lead to new and improved mechanistic basis for therapies and offer more effective treatment courses for these disease conditions.

To aid the understanding of the problem of pathological scarring in relation to keloids and FKN, it is therefore of importance to first understand the structure of the skin and associated appendages, and the normal wound healing responses. In the subsequent sections of the review of the literature we will be looking at an overview of skin structure then go on to the normal wound healing responses. Thereafter we will go into aberrant wound healing and

fibrogenesis and delve deeper into the two scarring diseases, Keloids and FKN. Subsequently we will then look at metabolism in relation to the two scarring diseases as well as the current treatment approaches, which will lead us into the problems associated with these treatments and the need for further research.

1.2. Skin structure

Being the largest organ of the human body, the skin is hence responsible for roughly 15% of the total body weight in adults. It comprises three layers: the epidermis, the dermis and the hypodermis/subcutaneous tissue which are the outer, central and innermost layers respectively. The origin of tissues in these three distinct layers is different and they converge producing this organ of high complexity (fig 1). The hypodermis/subcutaneous tissue and dermis originate from the mesoderm while the epidermis originates from the ectoderm[16].

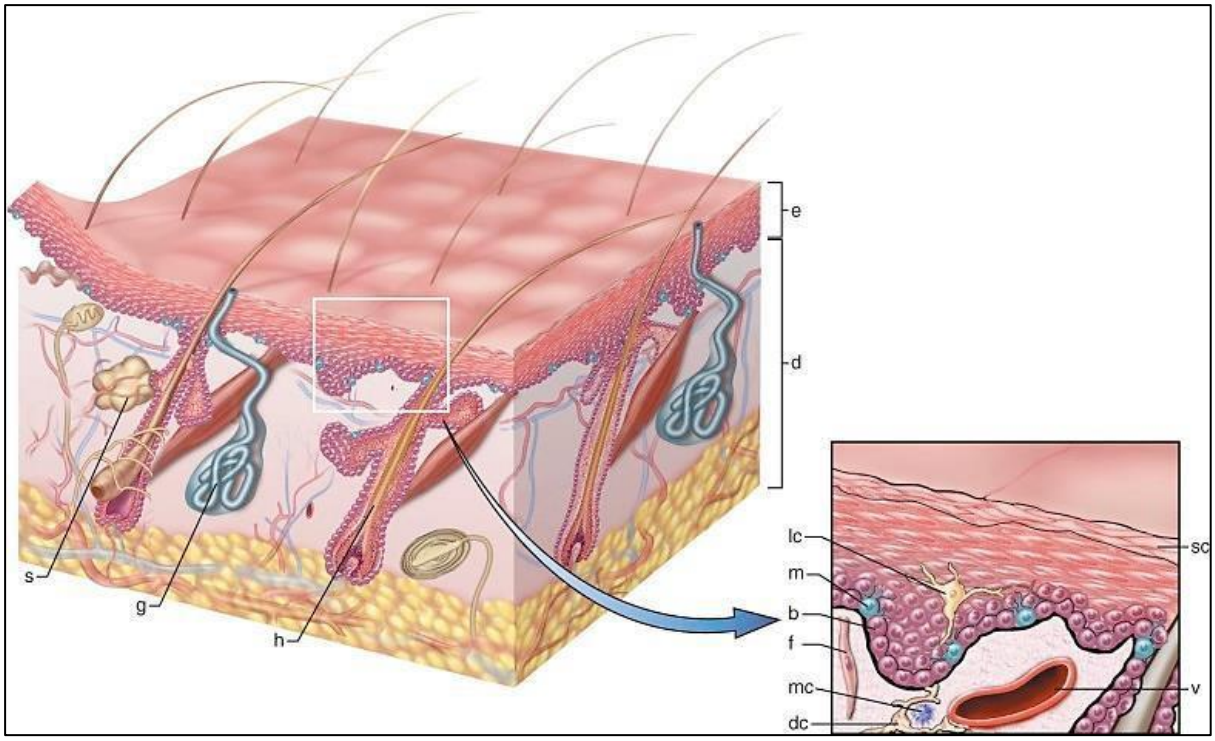

Figure 1.1. Cross section showing layers of human skin and appendages. Basal cell – b; dendrocyte - dc; dermis – d; epidermis - e; fibroblast – f; sweat gland - g; hair follicle - h; langerhans cell – lc; mast cell – mc; melanocyte – m; sebaceous gland – s; stratum corneum – sc; and blood vessel – v[17].

1.3. Progression of Wound Healing

After a wound occurs to the skin, a commencement of dynamic repair mechanisms immediately begins to close up the wound site. Wound healing gets derailed if this process of repair has an interruption, possibly leading to severe consequences. Pathological extremes that this may lead to include the development of excess scarring with subsequent keloid formation[18]. Usually occurring systematically in a very effective and proficient manner to regain normal anatomic structure, wound healing encompasses four recognizable phases that are overlapping but can be distinguished from each other. These are: (1) *Haemostasis*; (2) *Inflammation*; (3) *Proliferation*; and 4) *Remodelling* (fig 2).

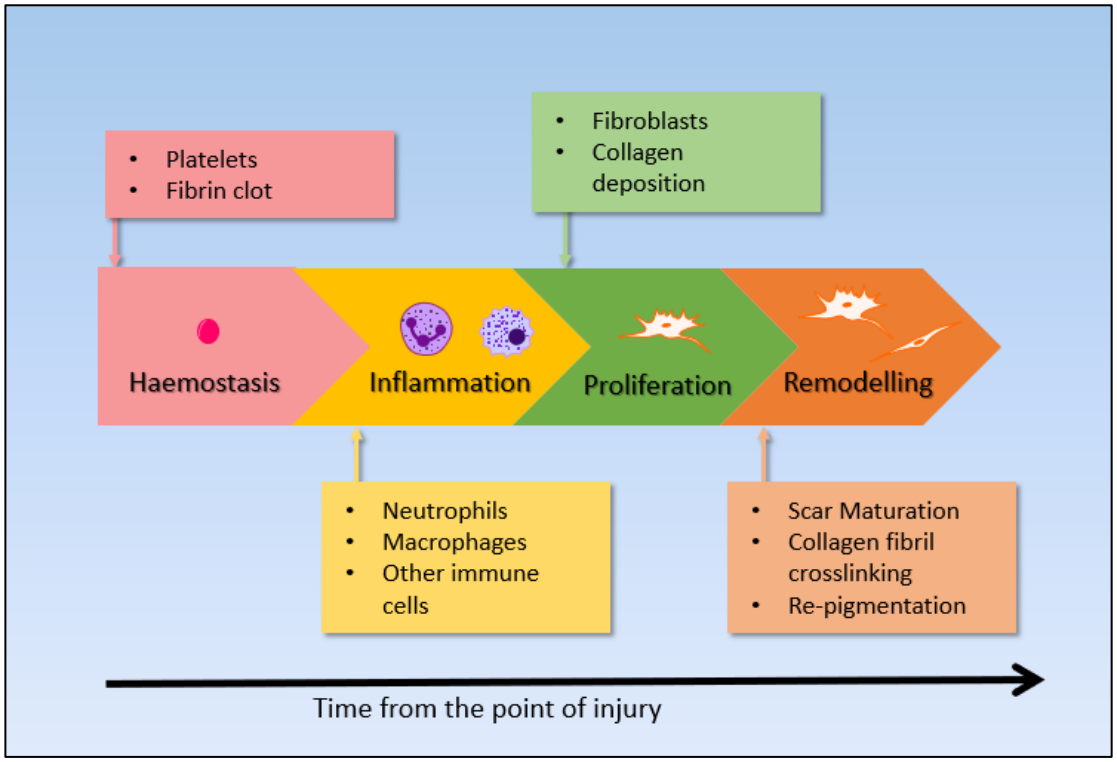

Figure 1.2. Summary of the overlapping phases of wound healing with some main features during each distinct phase. Adapted from Diegelmann *et al.*[19]

1.3.1. Haemostasis

This process is commenced as soon as the vasculature experiences damage and constituents of blood leak into the site of injury allowing an interaction between platelets and exposed collagen in addition to other components of the extracellular matrix[19]. The contact provokes the platelets and in a response they release growth factors that are essential to the wound

healing response as well as clotting factors. Additionally, they release cytokines such as platelet-derived growth factor (PDGF), Tumour necrosis factor alpha (TNF-α) and transforming growth factor beta (TGF-ß). The deposition of a blood clot consisting predominantly of extracellular proteins fibrin, fibronectin, thrombospondin and vitronectin is caused by this cytokine release. This clot functions to stop active bleeding at the wound site and further aids the healing process by acting as a provisional scaffold matrix to aid the migration of cells[20]. Moreover, vasoconstriction of the vessels is also simultaneously triggered by the platelets in the beginning of this phase. Haemostasis can range from a few seconds to hours[21]. Towards the end of haemostasis, platelets further cause vessel dilation and influence the infiltration of cells to the wound site via chemotactic attractants such as increased PDGF. This results in the infiltration of neutrophils, leukocytes, macrophages and fibroblasts (which via TGF-ß are later transformed into myofibroblasts). The platelets together with leukocytes then initiate the following process of inflammation through the release of interleukins[22].

1.3.2. Inflammation

During the inflammation stage, remnants of foreign substances in the wound, bacteria and tissue that has suffered damage begin to be phagocytosed by neutrophils. Mast cells are also attracted to the site and the complement cascade generates c3a and c5a anaphylatoxins which in addition to increasing blood vessel permeability, stimulate the mast cells into releasing leukotrienes and histamines. In addition to this, more macrophages infiltrate the wound site and together with the neutrophils continue the process of phagocytosis, and as a result increased amounts of TGF-ß and PDGF are released[23]. A positive feedback loop is generated as a result of the increased level of cytokines and in particular TGF-ß further causes the stimulation of wound macrophages. In response to this stimulation, these wound macrophages secrete more cytokines including interleukins (IL) 1, 6 and 8. They also secrete tumour necrosis alpha (TNFα) and fibroblast growth factor (FGF). In addition to aiding the process of chemotaxis, collagen and collagenase expression gets altered. Antimicrobial substances and proteinases also get released into the wound site to aid in the debridement[19,22]. Chemokines like CCL2 of the CC chemokine family aid monocyte chemotaxis to the wound where these cells differentiate into macrophages which helps remove apoptotic neutrophils and other dead cells. The inflammation phase can persist from hours to days[21].

1.3.3. Proliferation

After necessary phagocytosis to debride the wound site, the proliferation stage is initiated when fibroblasts infiltrate the site. These cells of mesenchymal origin are pivotal in the repair of the wounded tissue and start to produce and deposit collagen post migration and attachment to the provisional scaffold structure of the blood clot[20]. This results in the initiation of new extracellular matrix deposition. This occurs to cover up the wound site and addition to collagen type III, granulation tissue is also predominant at this stage[24]. As this phase of wound healing continues, re-epithelialization begins to occur led by keratinocytes and epithelial stem cells found in hair follicles in the bulge region as well as in sweat glands[25]. These cells produce cytokines which include epidermal growth factor (EGF), Insulin-like growth factor 1 (IGF-1) and vascular endothelial growth factor A (VEGFA) which results in the stimulation of endothelial cells. Moreover, wound macrophages are also stimulated and subsequently re-epithelialization begins[26,27].

VEGFA is required for the arrangement and assembly of endothelial cells into vascular structures in the processes of vasculogenesis and angiogenic remodelling that occur during re-epithelialization[28]. The process begins by sprouting of capillaries, and further breakdown of the hemidesmosomes and desmosomes results in the production of lipids that activate kinases attached to the membranes. This results in the membranes being more permeable to ions such as Calcium[22]. Innate lymphoid cells which are also resident in the skin were also shown to play a key role in the epithelialization process[29]. The keratinocytes are also responsible for the production of integrins, which aid in the attachment of the cell cytoskeleton to the other components of the extracellular matrix[30]. Melanocyte repopulation from the periphery of the wound site occurs at this point and trails keratinocytes. The proliferation phase goes on for days and can last up to a week[21].

1.3.4. Remodelling

During the final phase of remodelling, granulocytes undergo apoptosis to stop further granulation tissue from forming. Type III collagen that was initially deposited alongside granulation tissue is also replaced by type I collagen which is stronger[22]. This type I collagen is initially laid down in bundled parallel to each other and at this stage undergoes crosslinking. During this process components of the extracellular matrix (ECM)get continuously turned over as synthesis and degradation occurs. This degradation is carried out by ECM-degrading enzymes like matrix metalloproteinases (MMPs) which are also

produced by fibroblasts[31]. This is responsible for the intra- and inter-individual variation seen in the quality of scars. Consequently, this makes fibroblasts pivotal in the maintenance of the fibrillary ECM. They regulate the homeostasis that needs to be established and the structures as they regulate the ECM turnover[32]. Further melanocyte repopulation then results in re-pigmentation and hence a healed wound that continues to go through remodelling to regain normal structure and function of the site[33]. However, the exact role of melanocytes or their mechanisms of action during wound healing have not been extensively studied. The remodelling phase has a wide range lasting from as little as a week and can go on for several months[21].

1.4. Scar formation and Fibrogenesis

When an acute wound goes through the normal healing process, brief scar tissue comprising of newly haphazardly deposited collagen is formed, and this tissue continues to go through remodelling to regain normal structure and function. Wounds that have gone through the healing process without derailment of the process generally have skin that mirrors surrounding healthy tissue in texture as well as pigmentation[34]. When aberrant wound healing occurs, it can lead to permanent scars and fibrosis. In contrast to chronic ulcers which are in a constant state of inflammation, fibrogenesis occurs due to increased disproportionate levels of matrix deposition and reduction in remodelling. In addition to hypertrophic scars, the resulting excessive scarring can lead to conditions such as keloids[19] or Folliculitis Keloidalis Nuchae[6]. A number of factors have been reported to contribute to the formation of such scars. These include the race, age and type of skin the individual has, as well as the location, depth and treatment given to that particular wound[18].

1.5. Keloid Scars

1.5.1. Pathophysiology

Keloids are benign fibroproliferative growths with unknown aetiology and occur post trauma or a wound to the skin which includes piercings, surgery and thermal or chemical burns. They occur in susceptible individuals, with equal distribution between sexes, and are subsequent to a breakdown in normal wound healing responses. This malfunctioned response stems from an imbalance in the interplay between the phases of inflammation, proliferation and remodelling. Keloids are characterized by a dysregulation in the ratio of type I to type III collagen with a drastic increase in the amounts of not only type I collagen but the associated

glycoproteins as well during this aberrant wound progression[35]. A genetic predisposition to pathological scarring has been associated with keloids. These lesions don't exhibit regression and grow past the confines of the margin of the original wound and invade surrounding tissue[35,36]. They do not have a defined period of occurrence post injury and have been reported to be occur both relatively soon after the pathogenesis from which the scar arises or from a mature scar many years later[18]. Keloid scars have been reported in individuals as early as age 10 with an increase in the probability of getting keloids in the second and third decades of life, but a reduced probability post adolescence[37]. Clinically they present as slightly tender firm lumps with a glossy appearance. Hyperpigmentation is usually common and telangiectasia is sometimes present[38].

1.5.2. Histology

Histologically, keloids display a thickened epidermis that is flattened without rete ridges. In the dermis, heavily hyalinised collagen bundles of a random arrangement can be observed, and this results in the break-down of the distinct boundary between the papillary and reticular dermis. Additionally, skin appendages are displaced and ultimately destroyed[39]. Pro-inflammatory immune cells such as macrophages and lymphocytes were seen via immunohistochemistry to be persistent in keloid tissue. These cells are commonly known to be involved in chronic inflammation and are responsible for the release of cytokines and growth factors, which has led to the hypotheses that prolonged release of cytokines is responsible for the excessive cell proliferation and extracellular matrix deposition[22].

1.5.3. Genetics

There has been variation in the inheritance patterns of keloids with a large proportion being autosomal dominant. However keloid disease does not follow simple Mendelian single gene inheritance patterns but is more polygenic with linkage loci at chromosomes 2q23 and 7p11[40]. A study in a Japanese population identified 4 single nucleotide polymorphisms (SNPs) with two being in the same chromosomal region; rs940187 and rs1511412 at 3q22.3, rs873549 at 1q41 and rs8032158 at 15p21.3[41]. Another study in a Chinese Han population identified 3 SNPs in 2 chromosomal regions; rs2271289 at 15q21.3, rs873549 and rs1442440 at 1q41[42]. The two common regions identified in the two different populations suggests a commonality in the factors relating to the pathology of the disease in the East Asian

population[43]. This is yet to be done in an African population where keloids are also relatively common. Many studies have subsequently reported polymorphisms in fibrosis related genes with a large proportion including the transforming growth factor (TGF) pathway, others against decapentaplegic homologue (SMAD), epidermal growth factor receptor (EGFR) and human leucocyte antigen (HLA) alleles[43].

1.5.4. Factors affecting keloid formation

Keloids have been shown to be a multifactorial condition with many factors at play. These include firstly the collagen production amount. There was a 2- to 3-fold increase in the collagen synthesis and deposition rates of collagen in keloid fibroblasts versus normal fibroblasts in the same patients[44]. Secondly, keloid fibroblasts have been shown to have an upregulation in the receptors for the cytokines TGF-ß and platelet derived growth factor (PDGF) giving heightened sensitivity to growth factors[45]. Thirdly, in addition to an upregulation in the receptors they also display an upregulation in the expression levels of TGF-ß protein intracellularly[46,47]. Furthermore, a decrease in the expression of MMPs is linked to collagen synthesis and deposition rates as well as an increase in the production of other cytokines[48].

Other identified factors include the upregulation of the cell adhesion molecule and growth factor neuregulin-1 (NRG1) as well as the oncogene ErbB2 in the margin of keloid dermis. These have been suggested to work together in a pathway regulating the migration of keloid fibroblasts[49]. Lipid composition has also been implicated in keloid development. Some studies noted that there was about 60% increase in the triglycerides in keloids, irrespective of the fact that normal skin and keloids have similar ratios of fatty acids and cholesterol. This difference in lipids subsequently leads to differences in Eicosapentaenoic (EPA) and arachidonic acid (AA) cascades[50,51]. Moreover, lipids such as AA and diacylglycerol (DAG) are known to be second messengers interacting with lipid bundles of the cell membrane. This is important as mechanotransduction is a focal point in keloid formation[50].

Neuroimmune-endocrine circuits have also been implicated in keloid formation with a call for keloids to be included under psychophysiological disorders which include diseases such as psoriasis, seborrheic dermatitis and urticaria[52]. Psychological stress has been reported to be a risk factor for the reoccurrence of keloids in patients that underwent keloid surgical resection and postoperative radiotherapy. The patients were evaluated for psychological

stress on the day prior to the surgery and were evaluated at 3 month intervals for 12 months postoperatively[53].

It has been reported that keloid tissue, and more specifically keloid fibroblasts, exhibited higher levels of adenosine triphosphate (ATP) in comparison to other scars. Additionally, even up to 10 years post formation, there was still an increase in the numbers of fibroblasts in keloid tissue[54]. Interestingly, keloid fibroblasts have also been reported to exhibit augmented levels of fibroblast activation protein 1α (FAP-1α). This a molecular marker of activated fibroblasts but extensive research has not been done on FAP-1α in keloids[55]. This implies the significance of metabolism and bioenergetics in scar tissue.

Bioenergetics is the study of free energy transformation in living organisms. It encompasses the study of cellular processes like respiration as well as the metabolic and enzymatic pathways that are involved in the processing of energy sources to form utilizable energy such as ATP molecules in living organisms[56,57]. In addition to other studies that included the metabolism of keloids[58–60], a recent study by Li *et al*. has shown that keloid fibroblasts undergo metabolic reprogramming at the level of glycolysis. This has started to elucidate the precise metabolic phenotype of the cells in this condition[61].

1.6. Folliculitis Keloidalis Nuchae (FKN)

Folliculitis Keloidalis Nuchae (FKN) or Acne Keloidalis Nuchae (AKN) as it has commonly incorrectly been called, is a fibrotic condition that features chronic inflammation of the hair follicles with papule formation. The misdiagnosis is partly because of similar popular keloids as those seen in acne. However, the pathogenesis of FKN is not associated with increased production of sebaceous glands and the inflammation is not contributed by the presence of the bacteria *p. acnes* as occurs in acne. It has a 10 fold commonality in occurrence in males in comparison to females and affects mostly African men[62], but it has also been reported in Caucasian patients[63]. It is usually localized to the nuchal region of the scalp and the initially formed papules with exiting hair tend to merge to form prominent firm keloid like nodules and plaques eventually leading to scarring alopecia[6]. Pustules are also a common observation of this condition especially where there is active inflammation and/or infection[64]. Since its first description in the 1860s its exact aetiology is still unknown, and this may be due to very little research being carried out on the condition. It has been suggested that it is caused by ingrown hair as very close-shave cuts may initiate the

inflammatory process. This is based on the increased prevalence associated with joining the army and changes in popular hair styles (from the Afro's in the 1960-70's to clean-shaves since the 1990's) with similarities being made to Pseudofolliculitis barbae[65]. However, this has proven to be inconclusive as histological analysis from other investigators showed no ingrown hair present[6].

Some factors that affect the development and progression of FKN include: (1) trauma and repeated irritation to the occipital portion of the scalp during close haircuts; This has also been associated with bleeding during haircuts[62]; 2) seborrheic dermatitis[66]; and 3) elevated testosterone levels[66]

On account of the above factors and an increase in the amount of proteins produced by fibroblasts in the two disease conditions, this implies an abrogation of normal wound healing. This may be linked to failure to control the cells such as inflammatory cells involved during wound healing, or failure to downregulate wound healing responses after producing a healed wound[67]. Individuals that are prone to keloids or FKN do not always develop fibrotic lesions in response to wounding which is interesting as the fibroblasts in these individuals are considered anomalous. Selectivity to certain areas has been noted in the presentation of lesions in keloid patients with the chest, upper back and ears being more frequent[67]. FKN as prior stated is usually localized to the nuchal region of the scalp.

1.7. Pathological scarring and metabolism

In recent years, there has been a shift in focus to the metabolism in fibrotic conditions. During the process of metabolism, free energy is extracted from glucose which acts as a fuel source. This occurs via two main processes which are Glycolysis and Oxidative phosphorylation (OXPHOS). Glycolysis occurs in the cytoplasm of the cells while OXPHOS occurs in the Mitochondria using the products of Glycolysis; the main one being Pyruvate (Figure 1.3). This pyruvate then gets converted to Acetyl coenzyme A (CoA) which proceeds to enter the Krebs/Citric acid cycle producing electron carriers Nicotinamide adenine dinucleotide (NADH) and Flavin adenine dinucleotide ($FADH_2$) as well as some other intermediates. These electron carriers shuttle the electrons to the Electron Transport Chain (ETC) where OXPHOS occurs (Figure 1.4).

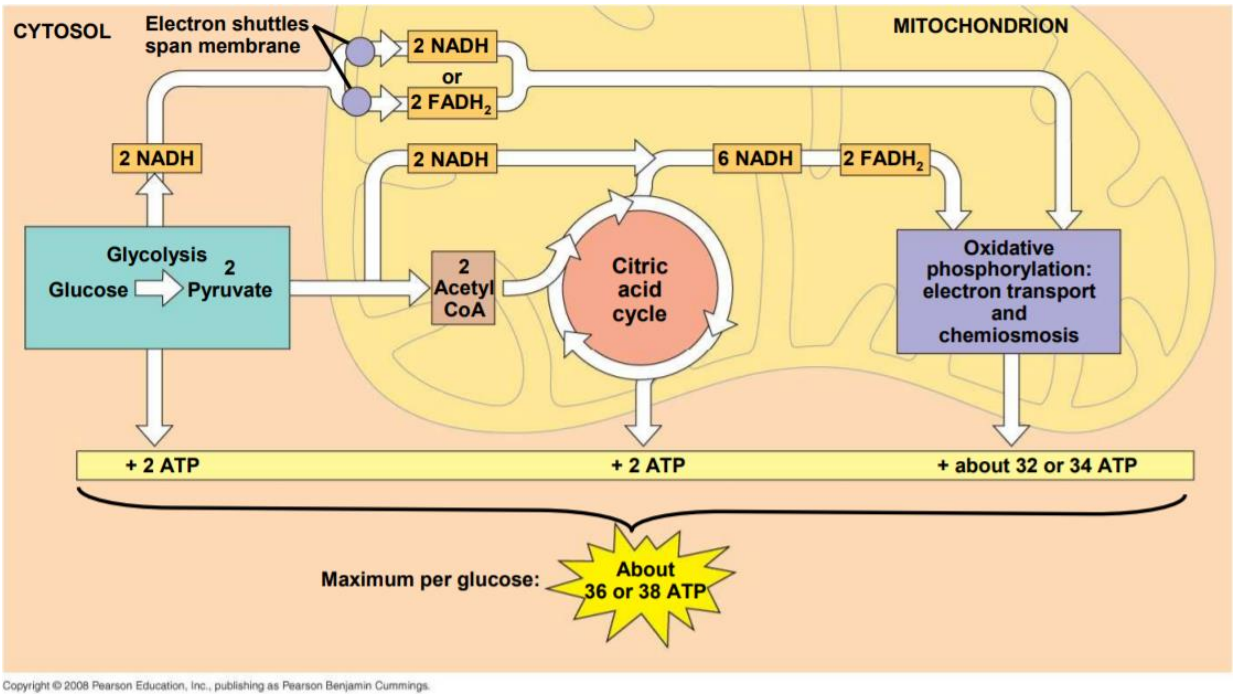

Figure 1.3. Overview of cellular respiration (Source: Campbell Biology)[68]

At the ETC electrons are shuttled through the 4 complexes with the aid of coenzyme Q and cytochrome C. As the electrons are passed from one complex to the next, protons are pumped out into the mitochondrial intermembrane space creating a chemiosmotic potential. These protons can only diffuse back into the mitochondrial matrix through ATP synthase which undergoes a change in configuration during the process producing ATP from ADP and an additional phosphate group (fig 1.4).

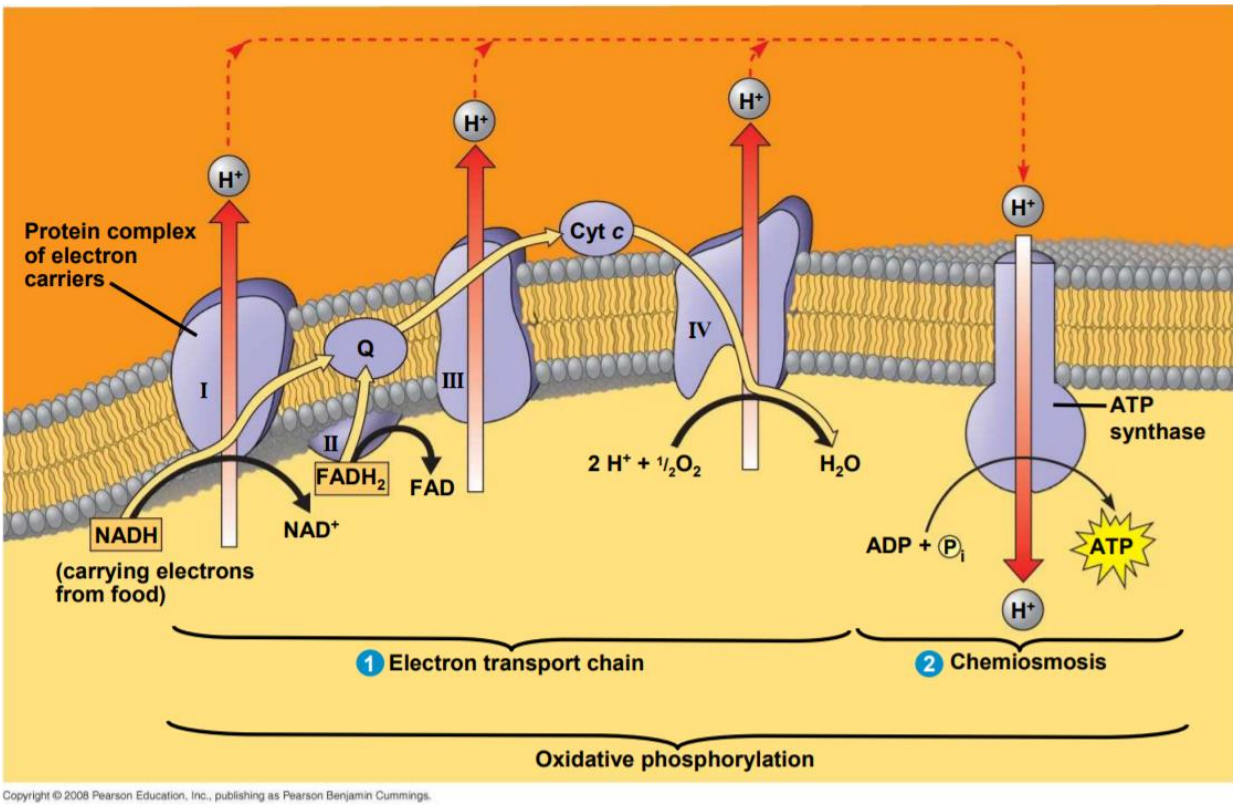

Figure 1.4. Oxidative Phosphorylation process (Source: Campbell Biology)[68]

Some studies have noted a disruption in the metabolism of fibrotic conditions such as Keloids. Liu *et al.*[58] showed using enrichment and pathway analysis following a microarray of gene expression in keloid tissue, that there was an upregulation in metabolism related genes. These included amino sugar and nucleotide sugar metabolism as well as oxidative phosphorylation genes. In another study, the unstable eicosanoid Prostaglandin D2 (PGD2) was shown to be increasingly metabolized to 9α,11β-PGF2 by the enzyme Aldo-keto reductase 1C3 (AKR1C3) which was upregulated in Keloids[59]. *Ozawa et al.*[60] showed using fluorine-18-fluorodeoxyglucose positron emission tomography (FDG-PET) that there was an accumulation of FDG which indicated an acceleration in glucose metabolism in keloids. However, more studies need to be done to better understand the problem of pathological scarring, with respect to metabolic perturbations.

1.8. Current approaches to treatment of Keloids

Everyday life and exposure to the elements makes avoiding wounding and as a result scarring that could be possibly pathological tremendously difficult, but in the event that an individual gets a wound, it is imperative that it is closed quickly and that there is no tension if it can be avoided[24]. Precaution should also be taken to ensure that foreign substances do not contaminate the wound where possible or the contamination is limited as this might exacerbate the problem leading to complicaions[67]. Highly inconsistent results on studies into keloids have plagued the numerous therapies proposed for keloids. Genetic and molecular biology tool advancements are now leading researchers to try prevent keloid formation by understanding the mechanisms underpinning the disease at a molecular level[38]. The most common forms of treatment for fibrosing scars like keloids include:

1.8.1. Compression therapy

In this treatment course, the first 6 months involve wearing specialized wound dressings. These dressings have the main purpose of applying pressure to the wound for a minimum of 8 hours each day. The premise of this therapy is that a constant supply of pressure to the wound prevents the formation of keloids but there has been no research into the exact mechanisms of action of this treatment[69].

1.8.2. Silicone therapy

Silicone sheeting and gels are used in an effort to minimize tension on the scar as well as to minimize the mobility. In this treatment course lasting a minimum of 2 months, a personal home care kit is usually supplied to the patient with silicone sheets/gels to be applied for at least half of the day. Silicone gels are used for areas where movement is usually unavoidable while for the more immobile areas silicone sheeting is used[70]. In similarity to compression therapy, there has been no concrete research into the understanding of the mechanism of action and further lacks proof of the influences that silicone therapy has on keloids at the molecular level.

1.8.3. Radiation therapy

This treatment course is usually used as an adjuvant therapy following surgical excision. Irradiation and electron beam radiation have been used and this is done to restore the delicate balance between the degradation and deposition of the ECM but has also showed varied results[71]. The mechanism of action that has been proposed for this treatment is that apoptosis

is induced in the excessively proliferating fibroblasts effectively reducing the fibroblast numbers of the lesion. As a result the scar can then undergo the normal process of remodelling and resolves with time[72].

1.8.4. Laser and photodynamic therapy

Laser therapy such as the carbon dioxide laser has shown to have some of the most varied results from a keloid therapy. In some cases there was very little to no improvement noted in more than half of the patients that underwent treatment[73]. Monthly treatments of the 585nm and 595nm wavelengths of the Pulsed dye laser (PDL) have also been studied[74]. Photodynamic therapy has also been used post sensitization with aminolaevulinic acid as well as with methyl aminolaevulinate[75].

1.8.5. Pharmacological therapies

Pharmacological therapies are usually the first line of treatment with steroids usually being used. Triamcinolone was one of the first corticosteroids used in the treatment of keloids due to its anti-inflammatory properties. Now more corticosteroids such as hydrocortisone, methyl-prednisolone and dexamethasone are being used[38]. The mechanism of action for corticosteroids is a reduction of collagen synthesis and an inhibition on the proliferation of fibroblasts. This is achieved through binding and altering the fibroblast gene expression[76]. More recently, drugs like Paclitaxel which have anti-fibrotic properties are being incorporated into nanoparticles and tested to improve the solubility and hence the effect of the drug[77].

1.8.6. Surgery and cryotherapy

The most effective and hence most common treatment option has been surgical excision of keloids. The keloid is removed in its entirety as well as a few millimetres of healthy normal tissue. Where a clear predisposition to keloids has been established, patients are particularly advised about re-occurrence[78]. In order to achieve the best possible results this therapy is used with other adjuvant therapies outlined above[79]. The most common synergistic therapy is intralesional corticosteroid injections of Triamcinolone into the keloid lesion. Cryotherapy with corticosteroid injections as an adjuvant therapy has gained more momentum in recent years as there have been reports on reduced reoccurrence rates but the therapeutic success is still varied[80].

1.9. Current approaches to treatment of FKN

FKN on the other hand has very limited research on treatment options for his disease. A recent systematic review highlighted medicinal treatment, surgical excision and light and laser therapy as the current treatment modalities for this disease[81].

1.9.1. Pharmacological therapy

Management of FKN using pharmacological therapy has included steroids, oral or topical antibiotics, and topical urea or fusidic acid[81]. Corticosteroid injections continue to be the most common treatment with the earliest case utilising intralesional triamcinolone and tetracycline[82]. Maintenance on low doses of oral isotretinoin has also been shown to improve inflammation of lesions with the best results being on the vertex of patient's scalp[83]. A combination of oral cefadroxil and fusidic acid has also been used, with prolonged antibiotic for up to 6 months before a marked improvement is seen[84].

1.9.2. Surgery

Surgical excision remains the most common form of management of FKN as it is the most effective at getting rid of the scars. This is done up to the deep subcutaneous tissue. Electrosurgery has been the most extensively studied and is preferred as it allows for simultaneous coagulation of small vessels limiting the bleeding. This is sometimes used with adjuvant therapies like topical and intralesional steroids[81,85].

1.9.3. Laser therapy

Various types of lasers have been utilised in treatment of FKN[81] with the earliest successful study using a CO_2 laser with a focused beam for surgical excision[86]. Ultraviolet B radiation has been used on FKN lesions with results showing a reduction of half the lesions over a 4month period[87].

1.10. The major problem associated with Keloid and FKN treatment

With all these current treatments, the underlying theme is that they are not effective at treating Keloids or FKN or preventing reoccurrence after excision. Additionally, they are not practical for day to day use as some require extended application of a treatment which may not be possible in certain environments such as the workplace. Consequently, there is still a need for better understanding of these fibrotic states to eventually improve and optimise treatment options that will lead to therapeutic success.

Recent studies utilising laser capture microdissection and transcriptomic array have shown that there are some site-specific differences in the genetic expression within the same keloid when the margin is compared to the centre[88]. Additionally, multipotent keloid-derived mesenchymal-like stem cells, which are cancer-like stem cells, have been suspected as well as reported in scalp keloids[88,89]. This could explain why completely successful and satisfactory therapies have been elusive for the treatment of these fibrotic states. Coupled with the reports on disruption in the metabolism of fibrotic conditions as well as the increase in ATP production of keloid tissue[54] and the FAP-1α marker[55], this further suggests the significance of the bioenergetic and metabolic activity changes that occur in scar tissue.

With these in mind, this study hypothesizes that bioenergetic changes that occur in keloid and FKN fibroblasts during states of pathological scarring play a significant role in fibroplasia and keloid formation via fibroblast activation.

1.11. Aims and Objectives

The aim of this project is to therefore investigate the disease phenotype of Keloid and FKN fibroblasts and establish whether these deviations from the normal state might be linked to or influence changes in bioenergetics in these fibroblast cells. This will include the following objectives:

Primary:

1. Culturing human dermal fibroblasts from skin biopsies of Keloids and FKN patients, as well as normal skin and normal scar controls

2. Analysis of the differences in fibroblast metabolism/energetics using extracellular flux measurements

3. Protein analysis using Western Blotting for the expression levels of proteins involved with bioenergetics already outlined in literature

Secondary:

4. Extracting RNA for future comparative RNA sequencing analysis of the genes involved in the bioenergetic pathway of fibroblasts as well as

5. Extracting DNA for future exome sequencing to identify differences in the genes in these conditions

CHAPTER 2. MATERIALS AND METHODS

2.1. Sample collection

Ethics approval for the study was granted by Groote Schuur Hospital and University of Cape Town's Human Research Ethics Committee. HREC REF No. 287/2018. Participants of this study consisted of consenting adult patients that were scheduled for Keloid or FKN surgical excision at the Outpatients Department of Plastic and Reconstructive Surgery unit of Groote Schuur Hospital. Additionally, consenting adult volunteers were used for normal skin and normal scar controls. This study was part of a larger study looking at different aspects of Keloids and FKN. For this portion of the study, 4mm punch biopsies were taken from all the participants for the culture of dermal skin Fibroblasts (Appendix A). For the Keloid disease, both perilesional and intralesional samples were collected to make comparative analysis between the two sites as reports have shown differential gene expression between the margin and the centre of the keloid[88]. Firm puritus regions were selected for FKN to avoid regions possibly undergoing active infection and inflammation. The punch biopsies were collected in Dulbecco's Modified Eagle's Medium (DMEM) (Life Technologies, SA).

2.2. Isolation of primary skin cells from tissue

Fibroblasts from the 2 disease conditions as well as the normal skin and normal scar controls were cultured from the 3mm skin punch biopsies. The skin tissue specimen first went thorough removal of the epidermis to separate melanocytes, keratinocytes and other cells found in the epidermis from the dermal tissue of interest. This was done through overnight incubation with 5mg/ml dispase at 4°C followed by peeling off the epidermis using forceps (B & M Scientifics, SA). Thereafter the remaining dermal tissue was cut up into small fragments using a scalpel blade (B & M Scientifics, SA) and underwent preparation for culture, which included washing with PBS and antibiotic treatment. The dermal tissue was then placed in 2 ml of culture medium comprising DMEM, 10% foetal bovine serum (Life Technologies, SA) with 1% penicillin-streptomycin antibiotic (Life Technologies, SA). The cultures were then maintained in a humidified incubator (WhiteSci, SA) at 37 °C with a 5% carbon dioxide atmosphere to allow growth of fibroblast cells. After sufficient outgrowth of these cells, they were sub-cultured for further experiments.

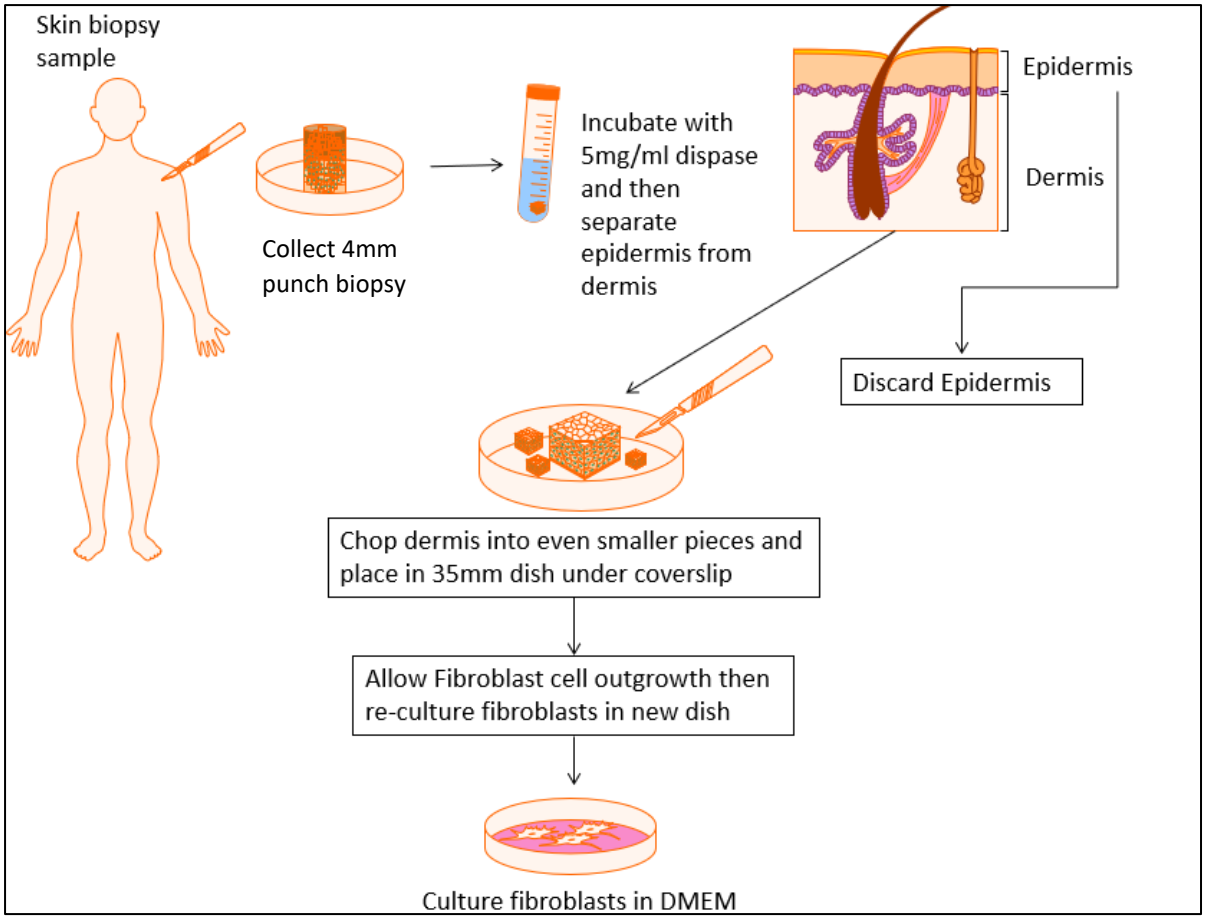

Figure 2.1. Summary of isolation and cell culture protocol of Human primary Fibroblast

2.3. Viability and Proliferation

To determine the cell growth dynamics in the different conditions, an xCELLigence Real Time Cell Analysis (RTCA) Instrument (ACEA Biosciences Inc., USA) was used. This instrument utilizes electrical impedance in specialized 8-well E-plates containing gold microelectrodes imprinted in each individual well. These microelectrodes are used to monitor the adhesion of cells and this is done by recording the electrical impedance that the cells cause in real time. Cells attaching to the microelectrodes cause a change in electronic readings which are output and plotted as cell index (CI) values, giving a precise indication of the viability and number of cells. Cells were then seeded at a density of 2 x 10^4 cells per well and the experiment was carried out for 4 days.

2.4. Fibroblast cellular migration

A 2-dimensional in vitro scratch motility assay was used as a wound healing model to investigate the migration profile of cells. Following culture of the cells to confluence in a 12-well culture plate, a scratch was made using a 10µL pipette tip through the monolayer. This was made to simulate a wound and a ruler was used to guarantee that consistent "wounds" across the stripped area were made. The medium was then replaced with 2ml of fresh medium to get rid of floating cells and debris that occurred from the scratching process. Thereafter, to prevent further proliferation of the cells a mitogen inhibitor, Mitomycin C (Sigma, USA), was then added at a final concentration of 0.1µg/µl. Across each scratch line, three marks were made on the underside of the dish to create reference points for taking images with an inverted light phase contrast microscope (EVOS, life Technologies, SA). Three images that spanned the length of the scratch that was made in each well of the tissue culture plate were then captured at the time of the scratch (denoted t = 0h). Subsequently, wound closure was monitored by the capture of images in a similar fashion at specified time points. For each of the three images captured at each time point, the area that was denuded was measured using Image J software (National Institutes of Health, USA) and the rate of migration was subsequently graphed:

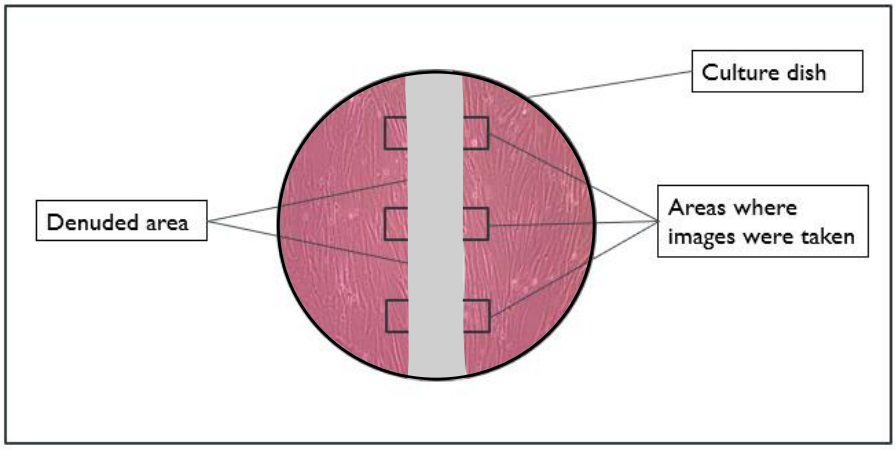

Figure 2.2. Scratch assay. Wound made using micropipette tip and monitored over time to determine the rate of wound closure by cell migration

2.5. Extracellular Flux analysis

Comparisons between the metabolic phenotypes of the cells from the disease conditions as well as the 2 control groups were then carried out. The Seahorse XFe96 Flux Analyser (Agilent Technologies, USA) which works based on the extracellular acidification rate (ECAR) and Oxygen consumption rate (OCR), was used for this purpose. The flux analyser utilises a sensor cartridge that monitors these two parameters.

2.5.1. Seahorse XF Cell Energy Phenotype Test

For this test, 20000 cells were seeded in a 96 well Seahorse tissue culture plate (Agilent Technologies). These cells were then left overnight to adhere in a 37°C CO_2 incubator. A sensor cartridge was placed in XF Calibrant fluid and also left to incubate overnight at 37°C in a non-CO_2 incubator. The following day, 1mM pyruvate, 2mM glutamine and 10mM glucose were supplemented to Seahorse XF Base medium to make assay medium. This prepared assay medium was pH adjusted to 7.4 and kept at 37°C until needed. The cell culture growth medium from the 96 well tissue culture plate was thereafter removed, and the cells were washed with warmed assay medium, before further addition of 180uL of assay medium to the wells. The tissue culture plate was then placed in a non-CO_2 incubator at 37°C for an incubation period of 45mins - 1 hour. A stressor mix consisting of a combination of Oligomycin (an inhibitor of ATP synthase) and Carbonyl cyanide-4 (trifluoromethoxy) phenylhydrazone (FCCP) (a mitochondrial uncoupling agent), was made up for addition to the tissue culture plate through injection ports on the previously incubated sensor cartridge during the assay. The loaded sensor cartridge was then placed over the tissue culture plate and the assay was consequently run for 2hrs as per the manufacturer's given instructions.

2.5.2. Seahorse XF Glycolytic Rate Assay

For this test, 20000 cells were seeded in a 96 well Seahorse tissue culture plate (Agilent Technologies). These cells were then left overnight to adhere in a 37°C CO_2 incubator. A sensor cartridge was also left to incubate overnight at 37°C in a non-CO_2 incubator. The following day, assay medium was first prepared by supplementing Seahorse XF Base medium with 1mM glutamine. This prepared assay medium was pH adjusted to 7.4 and kept at 37°C until the assay was run. The cell culture growth medium from the 96 well tissue culture plate was then removed, and the cells washed with warmed assay medium, before further addition of 180uL of assay medium. The tissue culture plate was then placed in a non-

CO_2 incubator at 37°C for an incubation period of 1 hour. The glycolysis stress test reagents, Oligomycin (ATP synthase inhibitor), Glucose and 2-deoxy-glucose (2-DG, which is a competitive inhibitor of glucose), were prepared for addition to the tissue culture plate during the assay through individual injection ports on the previously incubated sensor cartridge. The loaded sensor cartridge was then placed over the tissue culture plate and the assay was consequently run for 2hrs according to the manufacturer's instructions. The test reagents were injected in a sequential order during the assay; Firstly, Oligomycin, followed by Glucose, and finally the 2-DG.

2.5.3. Seahorse XF Cell Mito Stress Test

For this test, 20000 cells were seeded in a 96 well Seahorse tissue culture plate (Agilent Technologies). These cells were then left overnight to adhere in a 37°C CO_2 incubator. A sensor cartridge was placed in XF Calibrant fluid and also left to incubate overnight at 37°C in a non-CO_2 incubator. The following day, with 100mM pyruvate, 200mM glutamine and 2.5M glucose were supplemented to Seahorse XF Base medium to make assay medium. This prepared assay medium was pH adjusted to 7.4 and kept at 37°C until the assay was run. The cell culture growth medium from the 96 well tissue culture plate was then removed, and the cells washed with warmed assay medium, before further addition of 180uL of assay medium. The tissue culture plate was then placed in a non-CO_2 incubator at 37°C for an incubation period of 1 hour. Three stressor compounds were made up for addition to the tissue culture plate through individual injection ports on the previously incubated sensor cartridge during the assay. The stressors were FCCP (a mitochondrial uncoupling agent), Oligomycin (an inhibitor of ATP synthase) and a combination of Rotenone + antimycin A (inhibitors of complex I and III respectively of the ETC). The loaded sensor cartridge was then placed over the tissue culture plate and the assay was consequently run for 2hrs as per the instructions from the manufacturer. The stressors were injected in a sequential order during the assay; Firstly, FCCP, followed by Oligomycin, and finally the combination of Rotenone + antimycin A.

2.6. RNA, DNA and Protein Extraction

When cell cultures were confluent enough to give more than 1x10^6 cells, RNA, DNA and protein extraction was done using the Qiagen AllPrep DNA/RNA/Protein kit (WhiteSci, SA) as per the instructions form the manuacturer. Cells were trypsinized and pelleted before

resuspending in lysis buffer comprising buffer RLT containing β-mercaptoethanol in a ratio of 100:1 (Appendix B). The volume was dependent on the number of pelleted cells and the suspension was then vortexed for 1min. The mixture was then added to a DNA spin column and centrifuged for 30 seconds at > 10,000 rpm. The DNA spin column was kept for DNA isolation while the flow-through was used for RNA and protein extraction.

2.6.1. DNA

To the DNA spin column, 500µl of AW1 buffer was added and thereafter centrifuged for 15s at >10,000 rpm followed by a wash with AW2 buffer which was added and centrifuged for 2min at >10,000 rpm. The column was then placed in a 1.5ml collection tube and 50µl of EB buffer added, followed by a 1min incubation at room temp. This was then centrifuged at >10,000 rpm for 1min to elute the DNA. DNA then stored at -80 for future work.

2.6.2. RNA

To the flow-through, 400µl of 96% ethanol was added and mixed thoroughly by pipetting up and down. The mixture was then added to an RNA spin column and centrifuged for 15s at >10,000 rpm. The flow-through was kept for protein extraction, and 350µl of RW1 buffer was added to the RNA spin column and centrifuged for 15s at >10,000g followed by an intervening 80µl DNase1 incubation for 15min at room temp. Another 350µl of RW1 buffer was then added to the RNA spin column and centrifuged for 15s at >10,000 rpm. 500µl of RPE buffer was then added to the RNA spin column and centrifuged for 15s at >10,000 rpm, followed by a second 500µl wash with RPE buffer with centrifugation for 2min at >10,000 rpm. The RNA spin column was then placed in a 1.5ml collection tube and 30µl of RNase-free water was added to the column before incubation for 30s at room temp. The RNA spin column was then centrifuged for 1min at >10,000 rpm to elute the RNA. The RNA was then stored at -80 for future work.

2.6.3. Protein

To the flow-through from the 96% ethanol wash during the RNA extraction step, 600µl of APP buffer was added and mixed vigorously by pipetting and incubated for 10min at room temp. The mixture was then centrifuged for 10min at >10,000 rpm to pellet the precipitated protein, and the supernatant discarded. To the pellet, 500µl of 70% ethanol was added and centrifuged for 1min at >10,000 rpm with the subsequent supernatant being discarded. The pellet was then dried for 5-10min at room temp followed by addition of 240µl of HCL-Tris

buffer and vigorous mixing to dissolve the pellet. The mixture was then incubated at 95°C for 5min to completely dissolve and denature protein, then cooled to room temp before freezing at -20°C for future analysis.

2.7. Western Blotting

Fibroblast cell FAP-1α protein expression levels were analyzed using Western blotting for this study. This was to compare the induction of the protein in the two disease conditions in comparison to the controls.

2.7.1. Protein extraction and quantification

After extraction of protein with the Qiagen AllPrep kit as per the instructions from the manufacturer, the BCA assay was done for the protein concentrations to be established.

2.7.2. SDS-PAGE and transfer to nitrocellulose membrane

Subsequent to protein extraction, the protein samples were thereafter separated via electrophoresis on an SDS-PAGE gel comprising an initial 5% stacking gel on top of an 8% resolving gel (Appendix C). Prior to the loading of the gel, boiling blue buffer (Appendix C) in a ratio of 1:1 was added to the protein samples. This buffer aids the linearization of the proteins and gives them a negative charge as it contains SDS. In addition to containing a visualisation dye to help monitor the migration of the proteins through the gel, the boiling blue buffer also contains glycerol which aids the loading of the samples on the stacking gel. The boiling blue and protein sample mixture was then placed on a heating block for 5mins at 95°C. The molecular weight PageRuler Prestained Protein Marker (Fermentas, USA) was run in tandem with the samples in 1X running buffer (Appendix C) at 100V for 2 hours to establish the size of the proteins. For a loading control, unphosphorylated p38 which has a relatively high expression and stays constant in cells was used.

Following successful electrophoresis, a nitrocellulose blotting membrane (Amersham Hybond ECL; GE Healthcare, Germany) was used to transfer the resolved proteins. The nitrocellulose blotting membrane and the resolving gel underwent a 5min pre-soaking period in 1X transfer buffer (Appendix C). The nitrocellulose blotting membrane and the resolving gel were thereafter placed in the centre of a transfer “sandwich” cassette with Whatman filter paper and sponges on the fringes of both sides encasing them. This

"sandwich" cassette was then placed into the transfer tank of the Mini- PROTEAN Tetra Cell system (Bio-Rad Laboratories, USA) with the nitrocellulose blotting membrane on the positive side of the electrodes to ensure correct transfer of the proteins. The tank was filled with 1X transfer buffer (Appendix C) and the protein transfer done at 100V for 2hrs. Ice was used to keep temperatures low during the transfer.

2.7.3. Western blot detection

The membrane was rinsed with phosphate-buffered saline-tween (PBS-T) (Appendix C) following the transfer. This was followed by blocking of the membrane with 5% fat-free milk in PBS-T at room temperature for an incubation period of 1 hour. An overnight incubation with primary antibodies at 4°C with continuous shaking was then used to probe the membrane (Table 2.7). The membrane thereafter underwent 2 washes with PBS-T for 5mins each followed by 2 more washes for 10mins each, prior to incubation with the secondary antibody. This incubation was also carried out for 1 hour at room temperature. Subsequent to the incubation period, four washes (two for 5mins and two for 10mins as with the primary antibody) were done and the proteins were detected by the addition of WesternBright enhanced chemiluminescence (ECL) (Advansta, USA). Subsequent exposure of the membrane to x-ray film was then done to capture the chemiluminescent signal post 3min incubation with detection reagent which contains the Horseradish peroxidase substrate. The resulting blot was thereafter developed and fixed, and thereafter rinsed with water and air dried. Densitometry was carried out through normalization to the p38 loading control.

Table 2.7. Concentrations of antibodies used for Western blotting

Primary antibody	**Concentration**	**Secondary antibody**	**Concentration**
Rabbit polyclonal anti-FAP1α (Abcam, UK)	1:5000 in 5% fat-free milk	Goat anti-rabbit Horseradish peroxidase conjugate (Bio-Rad, USA)	1:5000 in 5% fat-free milk
Rabbit polyclonal antip38 (Sigma-Aldrich, USA)	1:5000 in 5% fat-free milk	Goat anti-rabbit Horseradish peroxidase conjugate (Bio-Rad, USA)	1:5000 in 5% fat-free milk

2.8. Statistical Analysis

Graphpad Prism (Version 6, Graphpad Software Inc.) was utilized for analysis of the raw data with results being expressed as means ± SEM. A One-way ANOVA with Tukey HSD post-hoc test was used for the comparison of groups of data sets. P-values less than: 0.05; 0.01 and 0.001 indicated statistically significant different values. All results are from data of at least 3 independent experiments each performed in triplicate.

Chapter 3. RESULTS

Fibroblasts from the 5 conditions used in this project and a summary of the main distinguishing features are outlined below (Table 3.1). The cells were sub-cultured and propagated for the various experiments.

Table 3.1 Morphological characteristics and features of fibroblasts under different conditions

Cell Type		**Distinguishing Features**
Normal Skin Fibroblasts (NS)	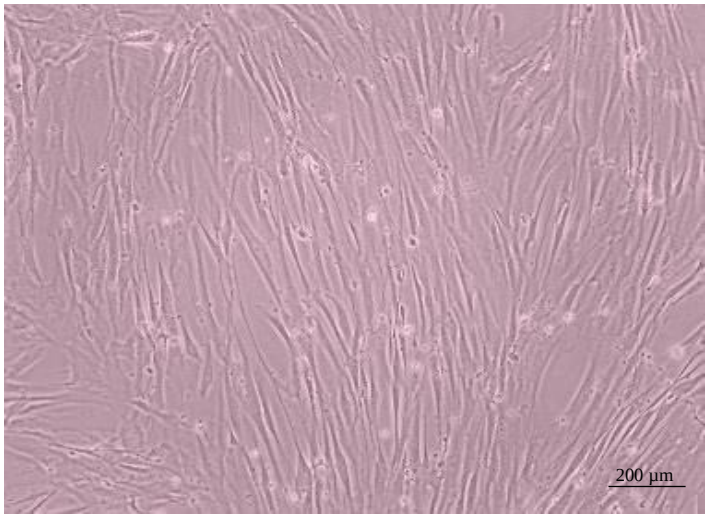	Elongated spindle shaped cells
Normal Scar Fibroblasts (NSc)	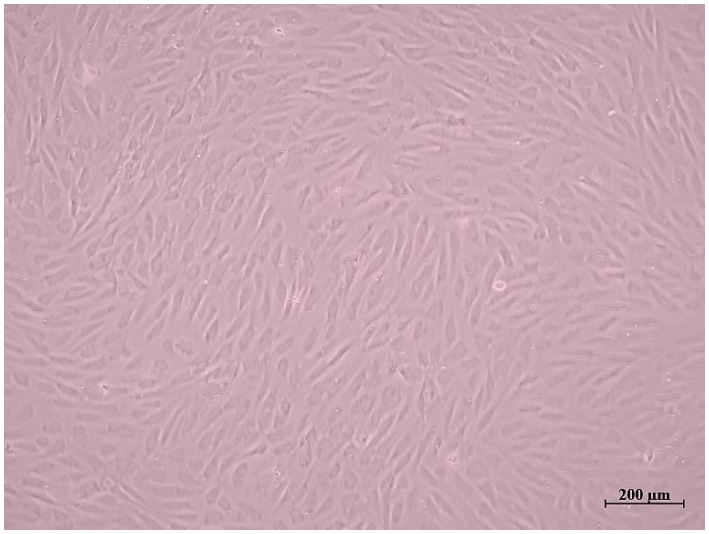	Relatively broad irregular flat shaped cells with short dendrites

Intralesional Keloid Fibroblasts (KI)	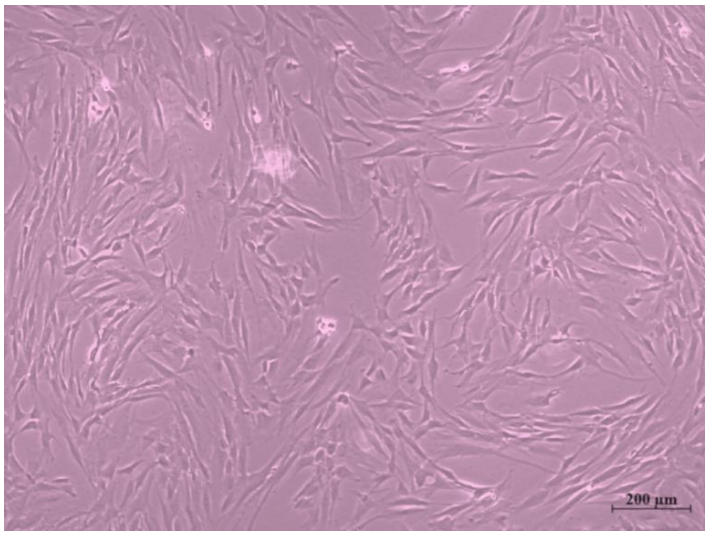	Irregular shaped cells that are relatively more stellate
Perilesional Keloid Fibroblasts (KP)	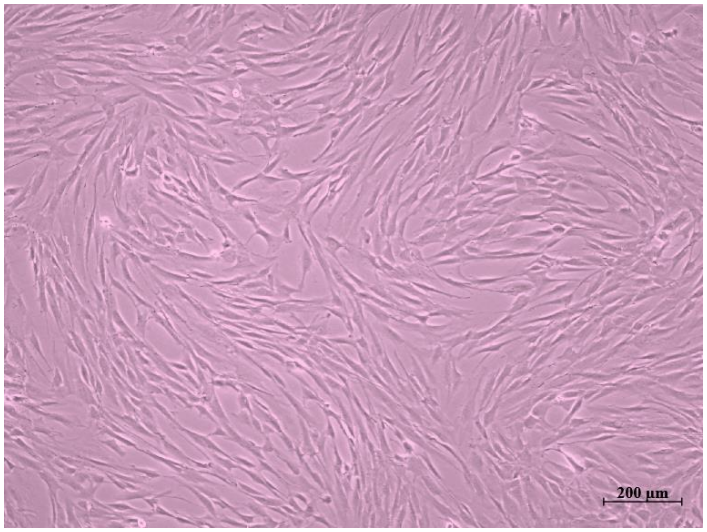	Morphologically similar to intralesional keloid fibroblasts
FKN Fibroblasts (FKN)	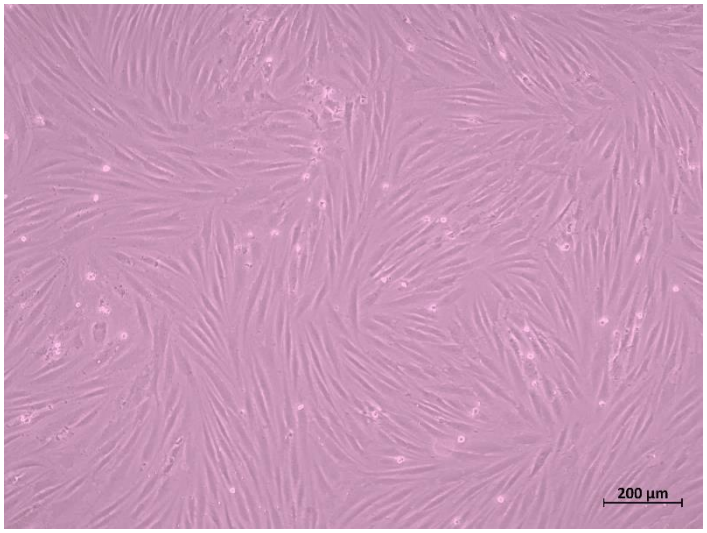	Tightly packing cells with slightly shorter dendrites than normal fibroblasts

3.1. Establishment of fibroblast cell growth dynamics in the different conditions

To begin to characterize the differences in cellular behaviour from the 5 conditions, first the proliferating ability of the cells was assessed. This was done to establish possible differences in their growth patterns. One of the clinically defining characteristics of keloids and FKN is their increased rate of collagen deposition. By looking at the proliferation of the different cells, inference could be made about whether it is a result of increased numbers of fibroblasts or whether similar numbers of fibroblasts are responsible for the collagen deposition in the conditions.

The inherent proliferation of the cells was measured in real time using an xCELLigence Real Time ell Analyzer (RTCA). To start, $1x10^4$ cells were plated per well of the RTCA plate and growth curves were constructed from these measurements over a 4-day period. As shown in figure 3.1 there were significant differences in the growth dynamics of the cells from the 5 different conditions. By the 72hr time point there was a marked increase in proliferation in the disease conditions relative to the controls as indicated by the cell index. After the 4-day period, the NS and NSc had mean cell indices of 5.36 ± 1.04 and 5.50 ± 0.54 respectively, whereas the keloid disease conditions had mean cell indices of 7.19 ± 0.21 and 7.79 ± 0.38 for KI and KP respectively. FKN had the highest mean cell index at 9.13 ± 0.25. Keloids and FKN had significantly higher proliferation than the controls, and it was further noted that FKN cells had a significantly higher proliferation than KI cells but not KP cells. There was no significant difference between the proliferation rates of the NS and NSc controls, and this was also noted between KI and KP as well even though KP was higher than KI.

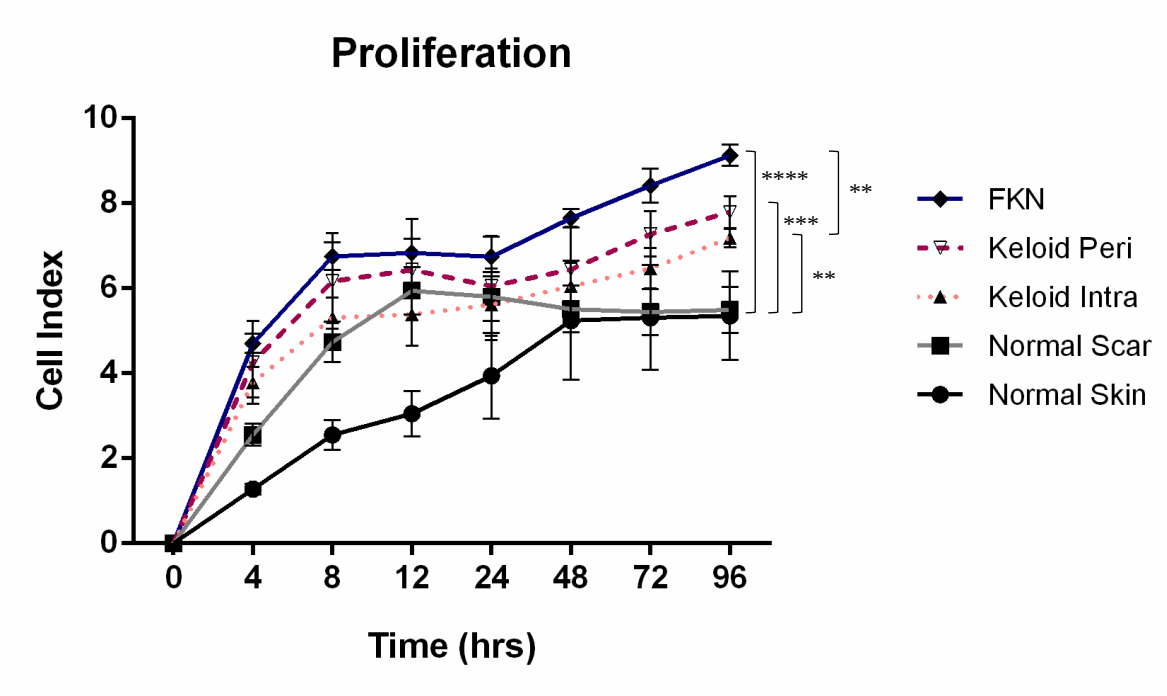

Figure 3.1. Inherent Fibroblast cellular proliferation. An xCELLigence RTCA instrument was used to measure the proliferation of the cells by growing cells in 10% FBS growth factor at a density of $1x10^4$ cells per well of the RTCA plate. Growth curves were conducted over a 4-day period. Results are representative of pooled data from 4 independent experiments with 2 replicates. Significance was set as *, $P < 0.05$; **, $P < 0.01$; ***, $P < 0.001$; ****, $P < 0.0001$; One-way ANOVA with Tukey HSD post-hoc test.

This therefore shows that Keloid and FKN fibroblasts exhibit increased proliferation capacity in comparison to controls.

3.2. Keloid fibroblasts show increase in migration ability while FKN fibroblasts have similar migration profile to controls

After the proliferating ability of the Fibroblasts in the different conditions was assessed, the migratory capacity was the next characteristic to be determined using scratch motility assays. After cell cultures were confluent, scratches were made through the monolayer to simulate a wound and the wound closure was measured and compared between the disease and control conditions. The percentage of the scratch closure relative to the size of the scratch area at time 0hrs was used to determine the area migrated (figure 3.2).

The results show that the average area migrated was significantly higher in both KI and KP fibroblasts at the 4hr and 12hr mark in comparison to the NS and NSc controls which had

similar migration profiles. At the 8hr mark only KP fibroblasts were significantly different to the controls.

Interestingly, FKN fibroblasts showed no significant difference in migration to the controls at all the time points, even though it followed a similar trend of an increase in migration at each time point.

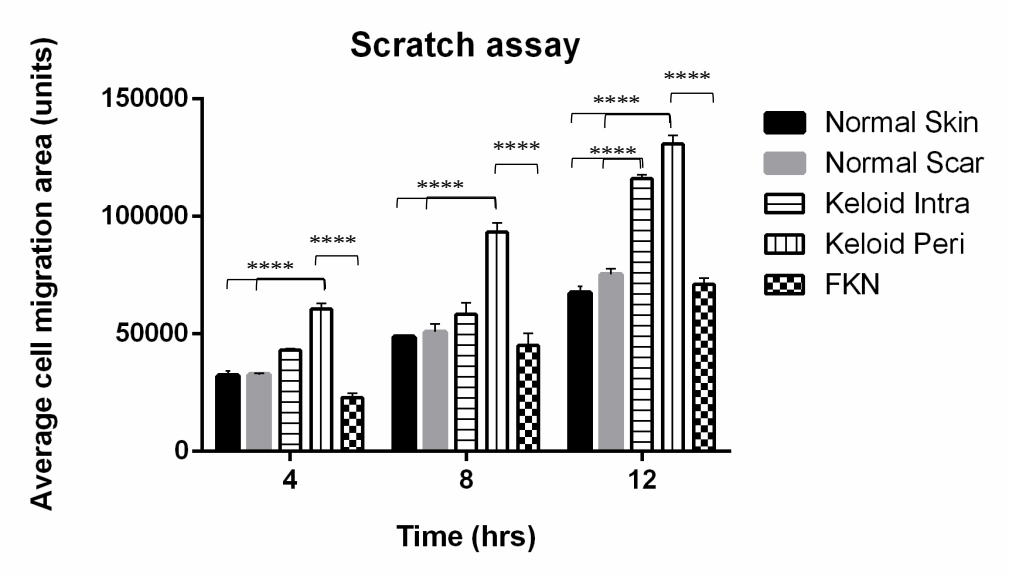

Figure 3.2. Scratch motility assays to determine migratory ability of fibroblasts. A two-dimensional motility assay was used to establish the migration. A linear wound was made by scratching through the monolayer with a pipette tip after cells were confluent. De novo cell proliferation was prevented by addition of Mitomycin-C (0.1µg/µl) and migration measured over a 12hr period. Keloids displayed increased migration. Results are representative of pooled data from 3 independent experiments with 3 replicates. Significance was set as *, $P < 0.05$; **, $P < 0.01$; ***, $P < 0.001$; ****, $P < 0.0001$; One-way ANOVA with Tukey HSD post-hoc test.

It is evident that both Keloid fibroblasts exhibit high migration rates, yet FKN fibroblasts exhibit normal migration capacity compared to other conditions and normal skin fibroblasts.

3.3. Keloid and FKN Fibroblasts have different energy phenotype profiles

Due to the differences in cellular behaviour that were observed, bioenergetic characterization experiments were then done in real time using the Agilent extracellular flux analyser. First, a cell energy phenotype experiment was carried out to see if there are basic differences in the energy phenotypes of the disease conditions relative to the controls. The Oxygen Consumption Rate (OCR) which acts as a proxy to mitochondrial respiration and Extracellular Acidification Rate (ECAR) which acts as a proxy to glycolysis, are measured under baseline and stressed conditions. This gives an indication of the metabolic potential of the cells.

As shown in figure 3.3A, there was a significant difference in the baseline OCR between the NS control and both the KI and KP fibroblast groups. The baseline OCR of the NS fibroblasts was 8.84 ± 0.22 pmol/min while KI was 31.37 ± 0.33pmol/min and KP was 41.78 ± 3.51pmol/min. The difference in baseline OCR was insignificant in the other groups. Under stressed conditions using an Oligomycin and Carbonyl cyanide-4 (trifluoromethoxy) phenylhydrazone (FCCP) mixture, the OCR increased and there was more than a 3-fold difference. The increment was to 13.56 ± 0.59pmol/min in NS fibroblasts, while it increased to 43.24 ± 5.00pmol/min in KI and 68.21 ± 6.63pmol/min in KP. There was also a significant difference between NS and FKN which increased to 48.28 ± 14.57pmol/min.

The baseline ECAR (figure 3.3B) shows a significant difference between NS 11.33 ± 0.84mpH/min and KP and FKN which are 25.56 ± 3.75mpH/min and 24.31 ± 2.68mpH/min respectively. After the Oligomycin and FCCP stressor mixture, there is a significant difference between NS and the other groups. The NS group ECAR increased to 19.19 ± 0.62mpH/min, while NSc 36.73 ± 1.39mpH/min, KI 36.57 ± 0.96mpH/min, KP 47.38 ± 7.72mpH/min and 47.68 ± 5.24mpH/min for FKN.

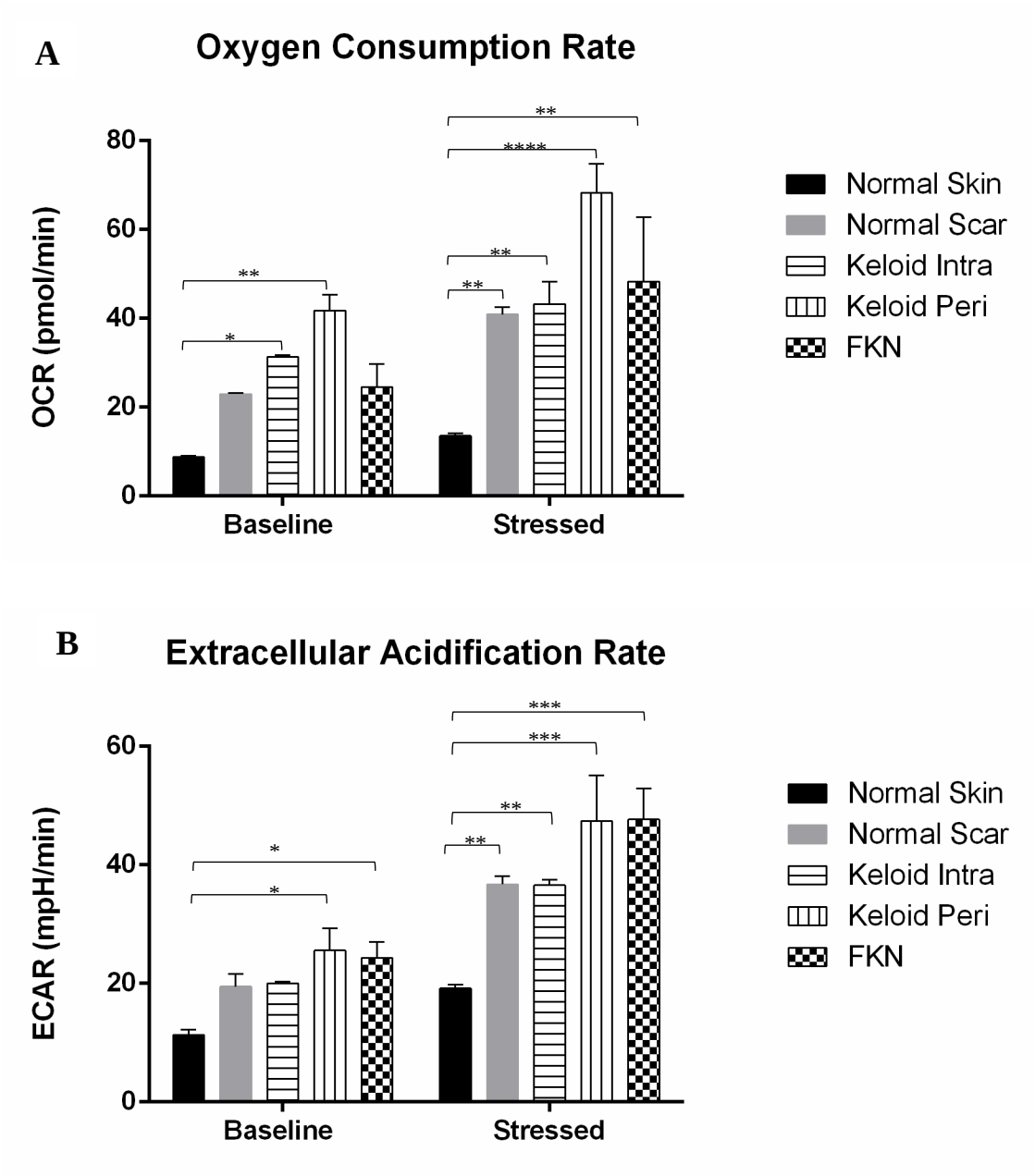

Figure 3.3. General cell energy phenotype. Results of Cell Energy Phenotype XF Flux analyser test for both A) OCR (pmol/min) and B) ECAR (mpH/min) simultaneously. Keloid and FKN fibroblasts showed increased metabolic potential. Results are representative of pooled data from 4 independent experiments with 3 replicates. Significance was set as *, $P < 0.05$; **, $P < 0.01$; ***, $P < 0.001$; ****, $P < 0.0001$; One-way ANOVA with Tukey HSD post-hoc test.

Therefore, Keloid and FKN Fibroblasts have different energy phenotype profiles.

3.4. Keloid and FKN Fibroblasts exhibit amplified glycolysis

Owing to the significant difference between controls and the disease conditions in basic energy phenotype experiments, the Agilent XF flux analyser Glycolysis Stress Test was used to further analyse the ECAR. This was done to determine whether the pathology of keloids involved the disruption of glycolytic pathways hence affecting glycolytic function. Cells were seeded and first observed under baseline conditions with subsequent injections of glucose, followed by Oligomycin and lastly 2-DG (figure 3.4A).

ECAR measured under baseline conditions is considered non-glycolytic acidification. It was significantly higher in KP and FKN, 9.45 ± 1.28mpH/min and 11.40 ± 0.95mpH/min respectively, in comparison to 6.85 ± 1.25mpH/min and 6.1 ± 0.80mp/min for NS and NSc respectively (figure 3.4B). Activation of glycolysis occurs after the addition of glucose and this is considered basal glycolysis. There was a significant difference between NS 16.80 ± 1.40mpH/min and KP and FKN, 25.00 ± 1.97mpH/min and 28.03 ± 2.34mpH/min respectively (figure 3.4C). After the Oligomycin injection to make glycolytic function maximal hence giving the overall glycolytic capacity, there was also a significant difference between NS 25.5 ± 0.60mpH/min and KP and FKN, 33.35 ± 3.55mpH/min and 50.17 ± 6.91mpH/min respectively (figure 3.4D). The glycolytic reserve which is the difference between the maximal and basal glycolysis was similar in all the groups except the FKN disease group where the glycolytic reserve was more than 2-fold higher than the other conditions (figure 3.4E). When 2-DG is injected, ECAR drops significantly to non-glycolytic levels because it acts as a non-competitive inhibitor of the glycolytic pathway.

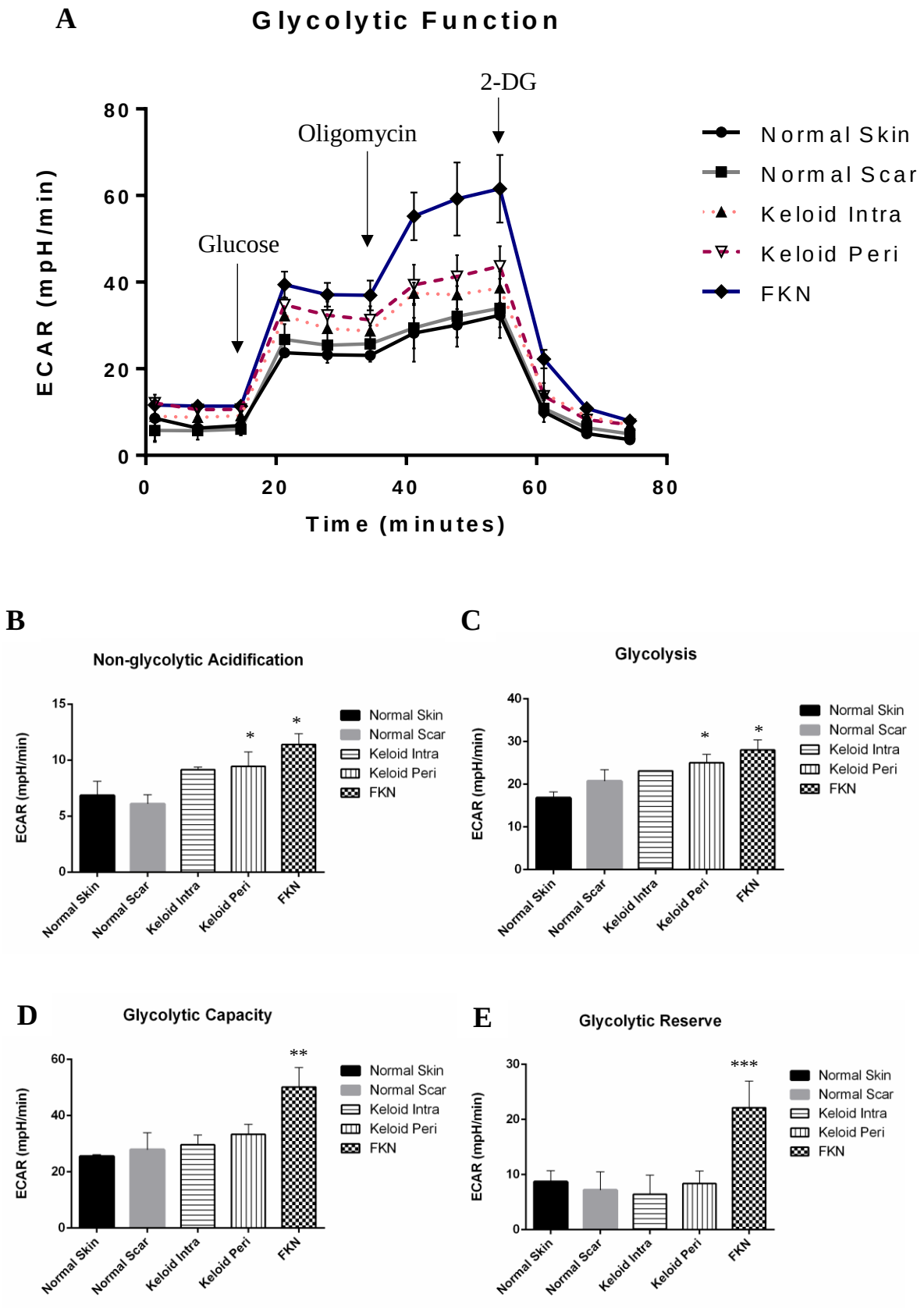

Figure 3.4. Bioenergetics parameters related to glycolysis. A) Profiles of Glycolysis Stress XF Flux analyser measurements of ECAR (mpH/min) in disease fibroblasts relative to

controls. Arrows indicate injection of glucose and the specific stressors into the media. B-E) Values of the different parameters of mitochondrial respiration. Keloid and FKN fibroblasts exhibit augmented glycolysis. Results are representative of pooled data from 4 independent experiments with 3 replicates. Significance was set as *, $P < 0.05$; **, $P < 0.01$; ***, $P < 0.001$; One-way ANOVA with Tukey HSD post-hoc test.

Evidently, Keloid and FKN Fibroblasts exhibit amplified glycolysis relative to the controls.

3.5. Keloid and FKN fibroblasts have Functional Mitochondria

Following the above results showing a shift towards glycolysis in Keloid and FKN fibroblasts, functional measurement of mitochondrial parameters was carried out to determine if the mitochondria in these fibroblasts were still functional. To do this, the Agilent XF Cell Mito Stress Test which looks at the OCR was used. Cells were seeded and first observed under baseline conditions with subsequent injections of Oligomycin, followed by FCCP uncoupling agent and lastly a Rotenone and Antimycin A inhibitor cocktail (figure 3.5A).

The results showed a significant increase in OCR measured under basal conditions in disease conditions relative to the controls. The basal respiration was the lowest in NSc at 19.7 ± 1.1pmol/min and was at 23 ± 1.4pmol/min in NS fibroblast cells. The Keloid fibroblasts had basal respiration rates of 26.5 ± 1.6pmol/min and 34.1 ± 2.3pmol/min for KI and KP respectively, while FKN had the highest basal respiration rate at 42.2 ± 2.5pmol/min (Figure 3.5B).

Following injection of the Oligomycin to determine ATP-linked respiration and proton leak, there was a significant difference in ATP-linked respiration between NSc 16.6 ± 0.8pmol/min and the disease conditions at 25.3 ± 0.9pmol/min and 32.3 ± 2.7pmol/min for KP and FKN respectively. There was no statistically significant difference between NS fibroblasts (20.0 ± 1.2pmol/min) and Keloids but a significant difference was recorded between NS fibroblasts and FKN. The proton leak was only significantly different between FKN at 9.8 ± 1.8pmol/min and the controls at 3.2 ± 0.4pmol/min and 3.1 ± 0.6pmol/min for NS and NSc respectively (Figure 3.5C-D).

Maximal respiration is established after injection of FCCP and a significant difference between the disease and control conditions was recorded. NS and NSc fibroblasts had maximal respiration rates of 43.9 ± 3.1pmol/min and 41.2 ± 2.3pmol/min respectively. In

comparison, KI was at 56.3 ± 5.7pmol/min, KP was at 67.3 ± 2.2pmol/min and FKN was almost double the controls at 80 ± 5.5pmol/min (Figure 3.5E). This gave the disease conditions a much higher spare respiratory capacity than the controls. The spare respiratory capacity is the difference between the maximal respiration and the ATP-linked respiration (Figure 3.5F).

After the Rotenone and Antimycin inhibitor cocktail injection, there is a rapid decrease in mitochondrial respiration as the mitochondrial processes are shut down (Figure 3.5A). This enables the quantification of the non-mitochondrial respiration which is a result of processes outside the mitochondria. The non-mitochondrial oxygen consumption was higher in the disease conditions in comparison to the controls although this difference was not statistically significant. The reverse was true for the coupling efficiency (Figure 3.5G-H).

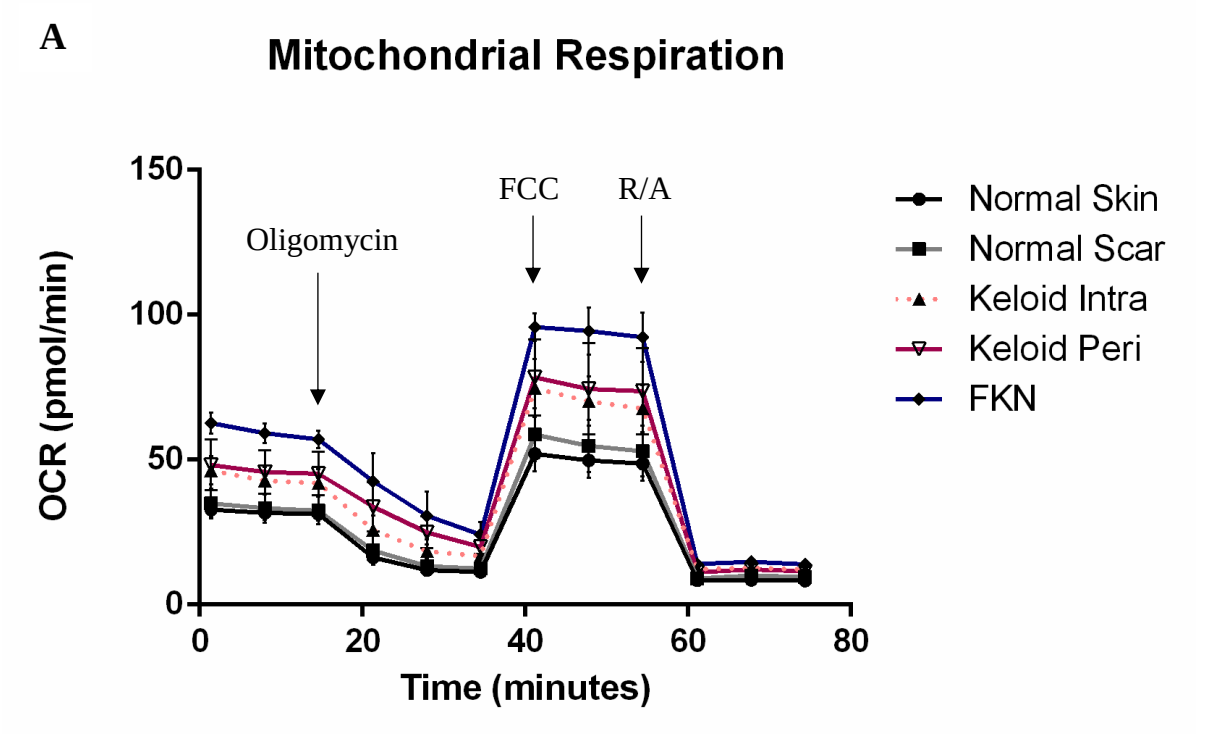

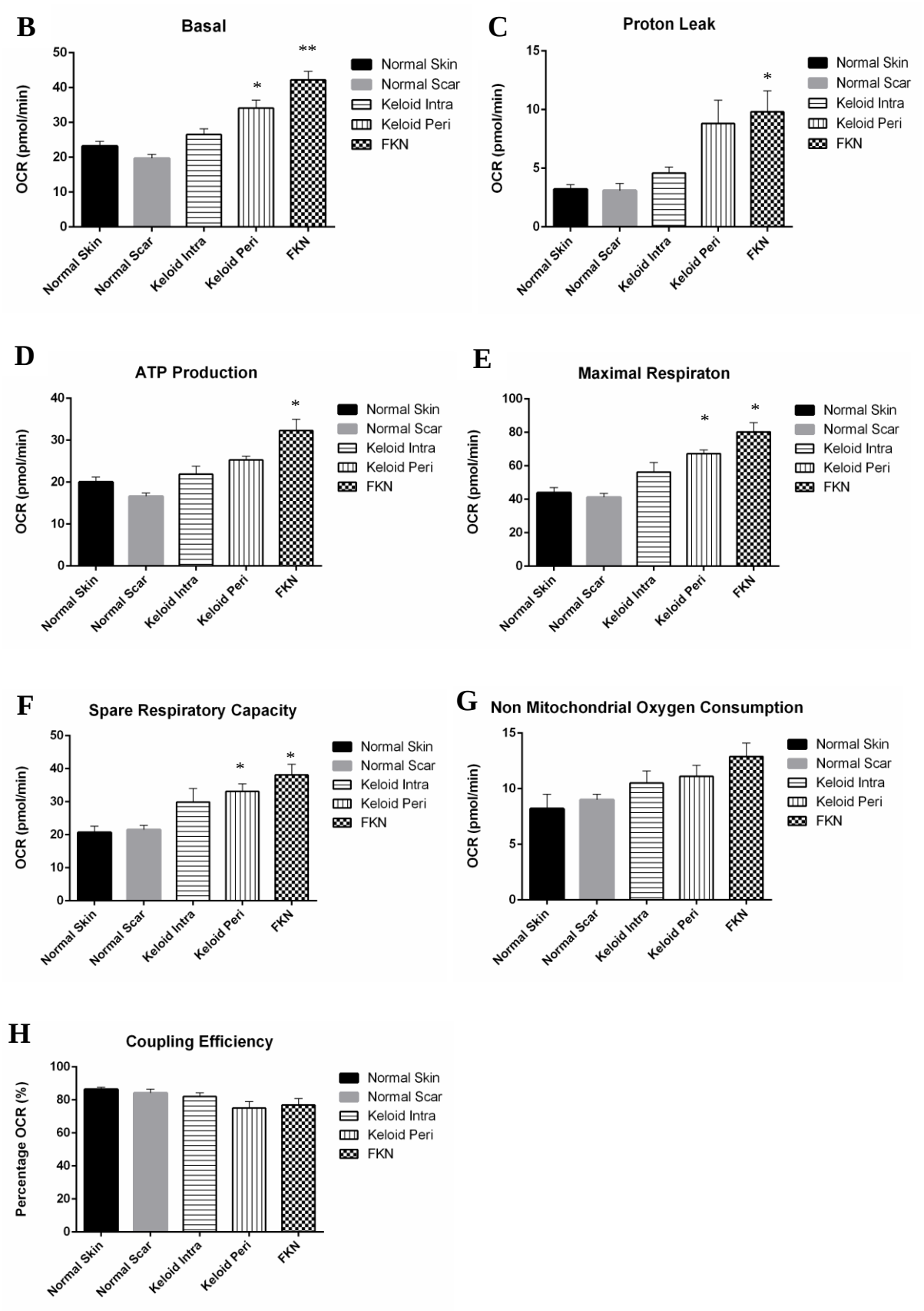

Figure 3.5. Bioenergetics parameters related to respiration in mitochondria. A) Profiles of Mito Stress XF Flux analyser measurements of OCR in disease fibroblasts relative to

controls. Arrows indicate injection of the specific stressors into the media. B-H) Values of the different parameters of mitochondrial respiration. Keloid and FKN fibroblasts have functional mitochondria capable of mitochondrial respiration. Results are representative of pooled data from 4 independent experiments with 3 replicates. Significance was set as *, $P < 0.05$; **, $P < 0.01$; ***, $P < 0.001$; One-way ANOVA with Tukey HSD post-hoc test.

Thus, Keloid and FKN fibroblasts also have functional Mitochondria.

3.6. Keloid and FKN fibroblasts produce significant amounts of FAP-1α protein

To begin to understand if the metabolic changes observed were associated with changes in proteins related to metabolism or activation states of the fibroblasts, expression of FAP-1α protein which has recently been reported to be upregulated in keloids was analysed. This was done by Western blotting which involved the extraction of whole cell proteins. The proteins were extracted subsequent to DNA and RNA extraction after cell cultures had been cultured to confluence. Unphosphorylated p38 which has a molecular weight of 38KDa and has a constant high expression was used as a loading control.

FAP-1α protein expression was found to be positive and significantly upregulated in both disease conditions relative to the normal skin and normal scar controls. The NS control fibroblasts showed negligible amounts of FAP-1α while NSc fibroblasts showed a slight increase although there was no statistically significant difference between them. On the other hand, the keloid fibroblasts showed a significant increase in FAP-1α expression with KI being 2-fold higher than NSc and KP being almost 3-fold higher. There was however no significant difference in expression levels between KI and KP fibroblasts. FKN showed the highest level of FAP-1α expression and was almost 4 times the expression levels in NSc fibroblasts.

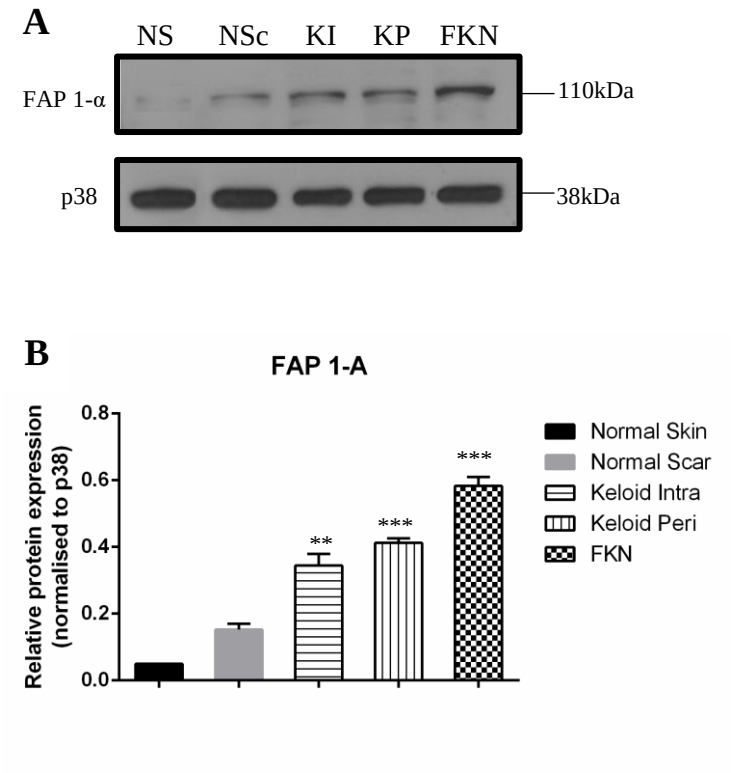

Figure 3.6. Expression of FAP-1α protein in Keloid ad FKN fibroblasts relative to controls. A) Western blot confirming the presence of FAP-1α in NSc, Keloid and FKN fibroblasts. Protein was harvested and analysed via SDS-PAGE. Primary antibodies to rabbit polyclonal FAP-1α and goat-anti-rabbit secondary antibody were used to quantify protein expression levels. B) Densitometry indicating relative protein expression of FAP-1α when normalised to p38 loading control.

Evidently, Keloid and FKN fibroblasts exhibit higher levels of FAP1-alpha compared to the controls, with FKN being even higher than Keloids.

Chapter 4. DISCUSSION

Keloids are benign fibroproliferative growths and occur after trauma or wounding of the skin, while Folliculitis Keloidalis Nuchae (FKN) is a fibrotic condition that features chronic inflammation of the hair follicles with papule formation[35,62]. These scarring diseases have devastating effects on the quality of life and current therapies are not effective at treating Keloids or FKN or preventing reoccurrence after excision. Consequently, there is still a need for better understanding of these fibrotic states to eventually improve and optimise treatment options that will lead to therapeutic success. The focus of the current study was to investigate the disease phenotype of Keloids and FKN at a cellular level and establish whether these deviations from the normal state might be linked to or influence changes in bioenergetics in fibroblast cells.

4.1. Establishment of fibroblast cell growth dynamics in the different conditions

To begin to determine differences in disease phenotype at the fibroblast level, first the proliferating ability of the cells was looked at using Real Time Cell Analysis. Growth curves performed over the 4-day period showed that both intralesional (KI) and perilesional keloid fibroblasts (KP) displayed an increase in proliferation relative to the normal scar (NSc) and normal skin (NS) controls with KP fibroblasts being higher than KI. The FKN fibroblasts showed an even higher increase in proliferation than both Keloid fibroblasts (Figure 3.1).

The difference in proliferation between KI and KP fibroblasts is presumably due to differences in gene expression and hence the proteins ultimately translated between the centre and the margin of the keloid. This is supported by a recent study that looked at the differential gene expression between the margin and the centre of keloids[88]. Clinically the margin is where the keloid mass is actively growing and invading normal skin, and this is in contrast to the centre which exhibits less growth. This suggests that the fibroblasts from the margin are in a more activated state in comparison to the centre.

As there are no published studies on the proliferation dynamics of fibroblasts in FKN, no comparison can be made to other studies. It is possible that certain unique genes or pathways are activated to produce the highly proliferative phenotype.

Interestingly, NSc fibroblasts showed a rapid increase in cell index which started to plateau early at the 48hr mark (Figure 3.1). At this point they undergo contact inhibition and stop

proliferating[90]. This rapid increase in cell index could be due to the larger size of the fibroblasts which are morphologically similar to a more senescent phenotype.

4.2. Keloid fibroblasts show increase in migration ability while FKN fibroblasts have similar migration profile to controls

The migration ability of the fibroblasts from the different conditions was also established. The scratch assay is used to measure the in vitro migratory ability of cells and is used as a wound healing model[91]. The results showed a significant increase in the migration of both KI and KP fibroblasts relative to the NS and NSc controls. FKN on the other hand exhibited a similar migration profile to the controls.

This is in agreement with other studies where significant increase in migration of Keloid fibroblasts has been reported[92,93]. This increase in migration may be attributed to upregulation in focal adhesion kinase which has been reported to be involved in mechanosensing during fibroblast migration[94] or an upregulation of matrix metalloproteinases[93].

Interestingly, FKN fibroblasts followed the general trend of the controls and there was no significant difference when compared to the controls. FKN is usually localised to the nuchal region of the scalp[62] and as such FKN fibroblasts may not exhibit increased migratory capacity relative to the controls. This implies that the cells may be less invasive in comparison to Keloid fibroblasts. FKN fibroblasts may have local proliferation which gives rise to the lesions that grow beyond the margins of injury as with keloids. However, as with the proliferation assays there have been no published studies on the migration of FKN fibroblasts.

4.3. Keloid and FKN Fibroblasts have different energy phenotype profiles

From the differences in phenotype observed after the proliferation and migration assays, a Cell Energy Phenotype test was performed. This test helps establish the metabolic potentials of the cells for Oxygen Consumption Rate (OCR) and Extracellular Acidification Rate (ECAR). It does this by comparing the baseline OCR and ECAR levels to the stressed levels after addition of a stressor cocktail.

The test showed a significant increase in baseline and stressed levels and of both OCR and ECAR, for the Keloid fibroblasts relative to the NS fibroblast control. This indicates overall

increased metabolic potential in keloid fibroblasts. FKN also exhibited a significant increase relative to the NS fibroblasts in all but the baseline OCR. The OCR is higher than NS fibroblasts under stressed conditions, so the data suggests that FKN fibroblasts have increased mitochondrial activity but may have an impairment to their overall mitochondrial metabolic potential as OCR is low under baseline. This has been established in other conditions like Late Onset Alzheimer's disease[95].

Unexpectedly, NSc fibroblasts also exhibited increased levels of both OCR and ECAR under stressed conditions to similar levels as KI fibroblasts. This suggests that NSc fibroblasts undergo some similar changes to their bioenergetic pathways even though the changes are not as extreme as in Keloids or FKN.

4.4. Keloid and FKN Fibroblasts exhibit amplified glycolysis

To further determine if glycolytic dysregulation and its potential effects on glycolytic flux is a factor in the transformed energy phenotype, the ECAR was measured via the Glycolysis Stress test (Figure 3.4A). ECAR is used as a substitute to measure lactate export which is an end product of glycolysis and is hence a proxy to monitoring glycolytic flux.

Baseline ECAR measurements were first taken indicating non-glycolytic acidification which was significantly higher in Keloid and FKN fibroblasts relative to the NS and NSc controls (Figure 3.4B). This shows that in the absence of glucose, the fibroblasts in these disease conditions produce more acid than the controls. When glucose gets injected, glycolysis is activated, and these are basal glycolytic levels (Figure 3.4C). The fibroblasts from the disease conditions have a higher increase relative to the controls showing that there are higher glycolysis basal levels in Keloid and FKN fibroblasts than NS and NSc controls. After addition of Oligomycin, mitochondrial respiration is shut down as it is an ATP synthase inhibitor. This creates an increase in glycolytic flux as the other energy source is blocked resulting in the maximum glycolytic capacity. The fibroblasts in the two disease conditions show a greater maximum glycolytic capacity than the controls, with FKN fibroblasts being significantly higher than keloid fibroblasts as well. Finally, 2-DG gets injected into the medium and glycolysis is blocked (Figure 3.4A) as 2-DG is a competitive glucose analogue that binds the hexokinase at the beginning of glycolysis. These results are supported by a recent study that also looked at Keloid cells and their metabolic reprogramming. An increase in glycolysis and the other glycolytic parameters was also recorded in their study[61].

Glycolytic inhibitors such as 3-Bromopyruvate which inhibits hexokinase activity hence abolishing ATP production, or Oxamic acid which inhibits lactate dehydrogenase, may be used[96].

4.5. Keloid and FKN fibroblasts have Functional Mitochondria

Due to the establishment of glycolytic dysregulation as a factor in the transformed energy phenotype, the study then went on to analyse the mitochondria and associated parameters of mitochondrial respiration. The OCR was measured via the Mito Stress test (Figure 3.5A). OCR is used as a proxy to monitoring mitochondrial respiration.

Baseline OCR measurements were first taken indicating basal respiration which was significantly higher in KP and FKN fibroblasts relative to the NS and NSc controls (Figure 3.5B). When Oligomycin gets injected, this leads to inhibition of ATP synthase and as a result creates a drop in OCR or mitochondrial respiration. This drop is indicative of ATP production in the mitochondria and the residual OCR is considered proton leak. ATP production (Figure 3.5D) was found to be higher in KP and FKN fibroblasts and proton leak (Figure 3.5C) was also significantly higher in these 2 disease fibroblasts. This supports suspicion of impairment to their overall mitochondrial metabolic potential alluded to in section 4.3 above. Interestingly, KP and FKN fibroblasts have the highest rate of proton leak, but at the same time they exhibit the highest ATP production as well as maximal respiration. This phenomenon could be due to increased mitochondrial numbers or size in these disease fibroblasts. This would account for the increased ATP production and maximal respiration exhibited. After addition of FCCP, this uncoupling agent collapses the mitochondrial membrane potential and electrons flow unimpeded through the electron transport chain. This results in maximal Oxygen to complex IV of the electron transport chain hence maximal OCR (Figure 3.5E) to give the spare respiratory capacity (Figure 3.5F). This spare capacity signifies the capabilities of the cell to withstand increased demand for energy and is higher in the disease conditions relative to the controls. The final injection is Rotenone and Antimycin A which block complexes I and III respectively allowing the determination of non-mitochondrial respiration[97].

Fibroblasts from the Keloid and FKN disease conditions had significantly higher spare respiratory capacities. This signifies that even though the fibroblasts from these disease conditions have functional mitochondria with even greater capacity for energy demand than

the controls, they utilise glycolysis. This switching to aerobic glycolysis is known as the Warburg effect and has been shown to be a hallmark of cancer cells[98]. It is a less efficient energy production mechanism and as such it's exact function has come into debate[99]. Many researchers have hypothesized the exact function of the Warburg effect, but the answer still remains vague. One prominent proposed function of this effect is that cells utilise it as an adaptive mechanism to support biosynthesis of molecules needed to aid the increased proliferation. Glucose gets used as a Carbon source during anabolism via the pathways that branch off of the main glycolytic pathway[100,101]. Oxidative stress due to the hypoxic environment of keloid fibroblasts has also been suggested as a reason for the Warburg effect, as a significant upregulation in the generation of ROS in keloid fibroblasts was noted[102]. These cells may switch to glycolysis as a defence mechanism against oxidative damage. FKN cells appear to be more competent in both glycolysis and mitochondrial respiration as shown by elevated levels of both OCR and ECAR after stressors. This may be the reason for their dramatically increased proliferation capacity as they utilise both energy metabolism pathways for their rapid multiplication solely to increase biomass and not to increase migration.

4.6. Keloid and FKN fibroblasts produce significant amounts of FAP-1α protein

In this study, we looked at Fibroblast Activation Protein-1α (FAP-1α) because it is a marker of activated states of fibroblasts. Due to increased activity and bioenergetics of the fibroblasts in the disease conditions, this can be inherently linked to the activation state of the fibroblasts. FAP-1α is a cell surface glycoprotein that is inducible and belongs to the serine protease group. It is transiently expressed in foetal mesenchymal cells but is usually not expressed in adult tissue[103,104]. Expression of FAP-1α gets induced in the reactive stroma of epithelial cancers and some sarcomas. In addition to this, it gets induced in activated fibroblasts reacting to wounding[105]. This protease has been shown to promote cell invasiveness as it is located on the cell surface membrane and a study by Dienus *et al.* showed an increase in FAP-1α expression in keloid fibroblasts in comparison to normal skin fibroblasts. The invasiveness of the Keloid fibroblasts was also reduced upon inhibition of the expression of FAP-1α[55]. This led us to further explore the expression of FAP-1α across all the conditions we had.

FAP-1α was found to be significantly positively expressed in normal scar tissue, as well as in both keloid (centre and margin) and FKN disease conditions. As FAP-1α gets induced in fibroblasts in wound healing states, it is likely that it would be positive in not only these

disease conditions but also in normal scar tissue as the process of remodelling may still be actively taking place. Although there are no published studies on FAP-1α in normal scar tissue or FKN, our findings in Keloids are supported by another study that had similar findings when they looked at FAP-1α expression in Keloids compared to normal skin[55].

CHAPTER 5. CONCLUSIONS

Altogether this study begins to give novel insight into the bioenergetics of normal scars and aberrant scarring diseases like FKN with no previously published data. Additionally, more insight is given into the bioenergetics of the centre and margin of the Keloid. There was an overall increase in the growth dynamics of disease fibroblasts compared to normal skin (NS) and normal scar (NSc) fibroblasts. While FKN fibroblasts show an increase in proliferation but no significant increase in migratory capacity, an increase in both parameters was observed in Keloid fibroblasts with the margin being higher that the centre. This increase in both proliferatory and migratory capacity may explain the higher local invasiveness of Keloids seen clinically relative to FKN. An overall increase in the bioenergetics was also observed in the disease fibroblasts in comparison to NS and NSc fibroblasts with a switch towards aerobic glycolysis. As attention to the changes that occur in the flux of metabolic pathways in oncogenesis has increased, similar research needs to be done in keloids and FKN as emerging research is showing stark similarities to some cancers. This can help improve therapies for Keloids and FKN which have been unsuccessful in the past or aid the creation of brand-new therapies. Drugs that have been previously used in cancer treatment may also be repurposed for the treatment of Keloids and FKN. Glycolytic inhibitors such as 3-Bromopyruvate and Oxamic acid may be used as a possible mechanistic basis for treatment.

Owing to the small tissue sample we could collect and trying to keep passage numbers minimal (cells only used up to passage 3) we were limited in the experiments we could perform. This study however, forms part of a larger study that is underway in our research group looking at different aspects of Keloids and FKN. Due to the heterogeneity of Keloid and FKN lesions, more participants need to be recruited and more tests run to get an even more precise picture of the disease conditions and to corroborate the novel findings. Comparison to a non-malignant (locally invasive) and malignant dermal cancer like Dermatofibrosarcoma Protuberans and Fibrosarcoma respectively, would likely yield more

understanding of the similarity to cancer. Tests like cell anchorage independent growth could be carried out as well as employing the use of cutting-edge technologies like In-cell Western blotting for in situ analysis of the cellular proteins. Furthermore, information from gene arrays or exome sequencing in addition to RNA sequencing would allow for targeting of genes and networks specific to the bioenergetic pathways that get dysregulated.

REFERENCES

1. Gao, F., Jin, R., Zhang, L. & Zhang, Y. The contribution of melanocytes to pathological scar formation during wound healing. *Int J Clin Exp Med* (2013).

2. Mari, W. *et al.* Novel Insights on Understanding of Keloid Scar: Article Review. *J. Am. Coll. Clin. Wound Spec.* **7**, 1–7 (2015).

3. Atiyeh, B. S., Costagliola, M. & Hayek, S. N. Keloid or hypertrophic scar: the controversy: review of the literature. *Ann. Plast. Surg.* **54**, 676–680 (2005).

4. Ud-Din, S. & Bayat, A. Strategic management of keloid disease in ethnic skin: a structured approach supported by the emerging literature. *Br. J. Dermatol.* **169**, 71–81 (2013).

5. Marttala, J., Andrews, J. P., Rosenbloom, J. & Uitto, J. Keloids: Animal models and pathologic equivalents to study tissue fibrosis. *Matrix Biol.* **51**, 47–54 (2016).

6. Sperling, L. C., Homoky, C., Pratt, L. & Sau, P. Acne keloidalis is a form of primary scarring alopecia. *Arch. Dermatol.* **136**, 479–484 (2000).

7. Reinholz, M. *et al.* The dermatology life quality index as a means to assess life quality in patients with different scar types. *J. Eur. Acad. Dermatology Venereol.* **29**, 2112–2119 (2015).

8. Froelich, K., Staudenmaier, R., Kleinsasser, N. & Hagen, R. Therapy of auricular keloids: review of different treatment modalities and proposal for a therapeutic algorithm. *Eur. Arch. Oto-Rhino-Laryngology* **264**, 1497–1508 (2007).

9. Alvarez, D. M. *et al. Defective Fatty Acid Metabolism Promotes Fibrosis in the Lung*.

10. Zhou, D. & Liu, Y. Understanding the mechanisms of kidney fibrosis. *Nat. Rev. Nephrol.* **12**, 68–70 (2016).

11. Vallée, A., Lecarpentier, Y., Guillevin, R. & Vallée, J.-N. Reprogramming energetic metabolism in Alzheimer's disease. *Life Sci.* **193**, 141–152 (2018).

12. Vallée, A., Lecarpentier, Y. & Vallée, J.-N. Thermodynamic Aspects and Reprogramming Cellular Energy Metabolism during the Fibrosis Process. *Int. J. Mol. Sci.* **18**, 2537 (2017).

13. Koppenol, W. H., Bounds, P. L. & Dang, C. V. Otto Warburg's contributions to current concepts of cancer metabolism. *Nat. Rev. Cancer* **11**, 325–337 (2011).

14. Hsu, P. P. & Sabatini, D. M. Cancer Cell Metabolism: Warburg and Beyond. *Cell* **134**, 703–707 (2008).

15. Pavlova, N. N. & Thompson, C. B. The Emerging Hallmarks of Cancer Metabolism. *Cell Metab.* **23**, 27–47 (2016).

16. Kanitakis, J. Anatomy, histology and immunohistochemistry of normal human skin. *Eur. J. Dermatology* **12**, 390–401 (2002).

17. Lazar, A. J. F. & Murphy, G. F. *Robbins and Cotran Pathologic Basis of Disease.* (Elsevier Health Sciences, 2015).

18. Bran, G. M., Goessler, U. R., Hormann, K., Riedel, F. & Sadick, H. Keloids: Current concepts of pathogenesis (Review). *Int. J. Mol. Med.* **24**, 283–293 (2009).

19. Diegelmann, R. F. & Evans, M. C. Wound healing: an overview of acute, fibrotic and delayed healing. *Front. Biosci.* **9**, 283–9 (2004).

20. Clark, R. A. F. Fibrin and wound healing. *Ann. N. Y. Acad. Sci.* **936**, 355–367 (2001).

21. Thiruvoth, F., Mohapatra, D., Sivakumar, D., Chittoria, R. & Nandhagopal, V. Current concepts in the physiology of adult wound healing. *Plast. Aesthetic Res.* **2**, 250 (2015).

22. Reinke, J. M. & Sorg, H. Wound Repair and Regeneration. *Eur. Surg. Res.* **49**, 35–43 (2012).

23. Lawrence, W. T. & Diegelmann, R. F. Growth factors in wound healing. *Clin Dermatol* **12**, 157–169 (1994).

24. Xue, M. & Jackson, C. J. Extracellular Matrix Reorganization During Wound Healing and Its Impact on Abnormal Scarring. *Adv. wound care* **4**, 119–136 (2015).

25. Roh, C. & Lyle, S. Cutaneous Stem Cells and Wound Healing. *Pediatr. Res.* **59**, 100R–103R (2006).

26. Ferrara, N., Gerber, H.-P. & LeCouter, J. The biology of VEGF and its receptors. *Nat. Med.* **9**, 669–676 (2003).

27. Schultz, G., Clark, W. & Rotatori, D. S. EGF and TGF-α in wound healing and repair. *J. Cell. Biochem.* **45**, 346–352 (1991).

28. Adams, R. H. & Alitalo, K. Molecular regulation of angiogenesis and lymphangiogenesis. *Nat. Rev. Mol. Cell Biol.* **8**, 464–478 (2007).

29. Rak, G. D. *et al.* IL-33-Dependent Group 2 Innate Lymphoid Cells Promote Cutaneous Wound Healing. *J. Invest. Dermatol.* **136**, 487–496 (2016).

30. Cavani, A. *et al.* Distinctive Integrin Expression in the Newly Forming Epidermis During Wound Healing in Humans. *J. Invest. Dermatol.* **101**, 600–604 (1993).

31. Parks, W. C. Matrix metalloproteinases in repair. *Wound Repair Regen.* **7**, 423–432 (1999).

32. Simian, M. *et al.* The interplay of matrix metalloproteinases, morphogens and growth factors is necessary for branching of mammary epithelial cells. *Development* **128**, 3117–31 (2001).

33. Snell, R. S. A study of the melanocytes and melanin in a healing deep wound. *J. Anat.* **97**, 243–53 (1963).

34. Lazarus, G. S. *et al.* Definitions and guidelines for assessment of wounds and evaluation of healing. *Wound Repair Regen.* **2**, 165–170 (1994).

35. Murray, J. C. Keloids and hypertrophic scars. *Clin. Dermatol.* **12**, 27–37 (1994).

36. English, R. S. & Shenefelt, P. D. Keloids and Hypertrophic Scars. *Dermatologic Surg.* **25**, 631–638 (1999).

37. Lane, J. E., Waller, J. L. & Davis, L. S. Relationship between age of ear piercing and keloid formation. *Pediatrics* **115**, 1312–4 (2005).

38. Al-Attar, A., Mess, S., Thomassen, J. M., Kauffman, C. L. & Davison, S. P. Keloid pathogenesis and treatment. *Plast. Reconstr. Surg.* **117**, 286–300 (2006).

39. Jumper, N., Paus, R. & Bayat, A. Functional histopathology of keloid disease. *Histol. Histopathol.* **30**, 1033–57 (2015).

40. Shih, B. & Bayat, A. Genetics of keloid scarring. *Arch. Dermatol. Res.* **302**, 319–339 (2010).

41. Nakashima, M. *et al.* A genome-wide association study identifies four susceptibility loci for keloid in the Japanese population. *Nat. Genet.* **42**, 768–771 (2010).

42. Zhu, F. *et al.* Association Study Confirmed Susceptibility Loci with Keloid in the Chinese Han Population. *PLoS One* **8**, e62377 (2013).

43. He, Y. *et al.* From genetics to epigenetics: new insights into keloid scarring. *Cell Prolif.* **50**, e12326 (2017).

44. Diegelmann, R. F., Cohen, I. K. & McCoy, B. J. Growth kinetics and collagen synthesis of normal skin, normal scar and keloid fibroblasts in vitro. *J. Cell. Physiol.* **98**, 341–6 (1979).

45. Haisa, M., Okochi, H. & Grotendorst, G. R. Elevated Levels of PDGF α Receptors in Keloid Fibroblasts Contribute to an Enhanced Response to PDGF. *J. Invest. Dermatol.* **103**, 560–563 (1994).

46. Babu, M., Diegelmann, R. & Oliver, N. Keloid Fibroblasts Exhibit an Altered Response to TGF-β. *J. Invest. Dermatol.* **99**, 650–655 (1992).

47. Chin, G. S. *et al.* Differential Expression of Transforming Growth Factor-β Receptors I and II and Activation of Smad 3 in Keloid Fibroblasts. *Plast. Reconstr. Surg.* **108**, 423–429 (2001).

48. Niessen, F. B., Spauwen, P. H., Schalkwijk, J. & Kon, M. On the nature of hypertrophic scars and keloids: a review. *Plast. Reconstr. Surg.* **104**, 1435–58 (1999).

49. Jumper, N., Hodgkinson, T., Paus, R. & Bayat, A. A Role for Neuregulin-1 in Promoting Keloid Fibroblast Migration via ErbB2-mediated Signaling. *Acta Derm. Venereol.* **97**, 675–684 (2017).

50. Clark, R. A. Cutaneous tissue repair: basic biologic considerations. I. *J. Am. Acad. Dermatol.* **13**, 701–25 (1985).

51. Huang, C. & Ogawa, R. Roles of lipid metabolism in keloid development. *Lipids Health Dis.* **12**, 60 (2013).

52. Hochman, B., Isoldi, F. C., Furtado, F. & Ferreira, L. M. New approach to the understanding of keloid: psychoneuroimmune-endocrine aspects. *Clin. Cosmet. Investig. Dermatol.* **8**, 67–73 (2015).

53. Furtado, F. *et al.* Psychological stress as a risk factor for postoperative keloid recurrence. *J. Psychosom. Res.* **72**, 282–287 (2012).

54. Ueda, K., Furuya, E., Yasuda, Y., Oba, S. & Tajima, S. Keloids Have Continuous High Metabolic Activity. *Plast. Reconstr. Surg.* **104**, 694–698 (1999).

55. Dienus, K., Bayat, A., Gilmore, B. F. & Seifert, O. Increased expression of fibroblast activation protein-alpha in keloid fibroblasts: implications for development of a novel treatment option. *Arch. Dermatol. Res.* **302**, 725–31 (2010).

56. Cox, M. M. & Nelson, D. L. *Lehninger principles of biochemistry.* (W H Freeman, 2013).

57. Green, D. E. & Zande, H. D. Vande. Universal energy principle of biological systems and the unity of bioenergetics (pairing principle/electronic energy release/enzymes as energy machines/thermodynamics of bond rupture). *Biochemistry* **78**, 5344–5347 (1981).

58. Liu, W. *et al.* Identification of Key Modules and Hub Genes of Keloids with Weighted Gene Coexpression Network Analysis. *Plast. Reconstr. Surg.* **139**, 376–390 (2017).

59. Mantel, A., Newsome, A., Thekkudan, T., Frazier, R. & Katdare, M. The role of aldo-keto reductase 1C3 (AKR1C3)-mediated prostaglandin D2 (PGD2) metabolism in keloids. *Exp. Dermatol.* **25**, 38–43 (2016).

60. Ozawa, T. *et al.* Accumulation of glucose in keloids with FDG-PET. *Ann. Nucl. Med.* **20**, 41–44 (2006).

61. Li, Q. *et al.* Metabolic reprogramming in keloid fibroblasts: Aerobic glycolysis and a novel therapeutic strategy. *Biochem. Biophys. Res. Commun.* **496**, 641–647 (2018).

62. Khumalo, N. P., Gumedze, F. & Lehloenya, R. Folliculitis keloidalis nuchae is associated with the risk for bleeding from haircuts. *Int. J. Dermatol.* **50**, 1212–1216 (2011).

63. Azurdia, R. M., Graham, R. M., Weismann, K., Guerin, D. M. & Parslew, R. Acne keloidalis in caucasian patients on cyclosporin following organ transplantation. *Br. J. Dermatol.* **143**, 465–7 (2000).

64. Alexis, A., Heath, C. R. & Halder, R. M. Folliculitis Keloidalis Nuchae and Pseudofolliculitis Barbae: Are Prevention and Effective Treatment Within Reach? *Dermatol. Clin.* **32**, 183–191 (2014).

65. Smith, J. D. & Odom, R. B. Pseudofolliculitis Capitis. *Arch. Dermatol.* **113**, 328 (1977).

66. George, A. O., Akanji, A. O., Nduka, E. U., Olasode, J. B. & Odusan, O. Clinical, biochemical and morphologic features of acne keloidalis in a black population. *Int. J. Dermatol.* **32**, 714–716 (1993).

67. Slemp, A. E. & Kirschner, R. E. Keloids and scars: A review of keloids and scars, their pathogenesis, risk factors, and management. *Curr. Opin. Pediatr.* **18**, 396 – 402 (2006).

68. Reece, J. B., Cain, M. L., Wasserman, S. A., Minorsky, P. V & Jackson, R. B. Cellular respiration and fermentation. in *Campbell Biology* 163–183 (Benjamin Cummings, 2011).

69. Kischer, C. W., Shetlar, M. R. & Shetlar, C. L. Alteration of hypertrophic scars

induced by mechanical pressure. *Arch. Dermatol.* **111**, 60–4 (1975).

70. Fulton, J. E. Silicone gel sheeting for the prevention and management of evolving hypertrophic and keloid scars. *Dermatologic Surg.* **21**, 947–951 (1995).

71. Malaker, K., Vijayraghavan, K., Hodson, I. & Yafi, T. Al. Retrospective analysis of treatment of unresectable keloids with primary radiation over 25 years. *Clin. Oncol.* **16**, 290–298 (2004).

72. Tosa, M. *et al.* Global Gene Expression Analysis of Keloid Fibroblasts in Response to Electron Beam Irradiation Reveals the Involvement of Interleukin-6 Pathway. *J. Invest. Dermatol.* **124**, 704–713 (2005).

73. Norris, J. E. The effect of carbon dioxide laser surgery on the recurrence of keloids. *Plast. Reconstr. Surg.* **87**, 44–49 (1991).

74. Kono, T., Erçöçen, A. R., Nakazawa, H. & Nozaki, M. Treatment of hypertrophic scars using a long-pulsed dye laser with cryogen-spray cooling. *Ann. Plast. Surg.* **54**, 487–493 (2005).

75. Mendoza, J. *et al.* Differential cytotoxic response in keloid fibroblasts exposed to photodynamic therapy is dependent on photosensitiser precursor, fluence and location of fibroblasts within the lesion. *Arch. Dermatol. Res.* **304**, 549–562 (2012).

76. Kauh, Y. C. *et al.* Major suppression of pro-α1(I) type I collagen gene expression in the dermis after keloid excision and immediate intrawound injection of triamcinolone acetonide. *J. Am. Acad. Dermatol.* **37**, 586–589 (1997).

77. Wang, M. *et al.* Improving the anti-keloid outcomes through liposomes loading paclitaxel–cholesterol complexes. *Int. J. Nanomedicine* **Volume 14**, 1385–1400 (2019).

78. Lee, Y., Minn, K. W., Baek, R. M. & Hong, J. J. A new surgical treatment of keloid: keloid core excision. *Ann. Plast. Surg.* **46**, 135–40 (2001).

79. Berman, B. & Bieley, H. C. Adjunct Therapies to Surgical Management of Keloids. *Dermatologic Surg.* **22**, 126–130 (1996).

80. Schwaiger, H., Reinholz, M., Poetschke, J., Ruzicka, T. & Gauglitz, G. Evaluating the Therapeutic Success of Keloids Treated With Cryotherapy and Intralesional Corticosteroids Using Noninvasive Objective Measures. *Dermatol. Surg.* **44**, 635–644 (2018).

81. Maranda, E. L., Simmons, B. J., Nguyen, A. H., Lim, V. M. & Keri, J. E. Treatment of Acne Keloidalis Nuchae: A Systematic Review of the Literature. *Dermatol. Ther. (Heidelb).* **6**, 363–78 (2016).

82. Dinehart, S., Tanner, L., Mallory, S. & Herzberg, A. Acne keloidalis in women. *Cutis* **44**, 250–252 (1989).

83. Goh, M. S., Magee, J. & Chong, A. H. Keratosis follicularis spinulosa decalvans and acne keloidalis nuchae. *Australas. J. Dermatol.* **46**, 257–260 (2005).

84. Janjua, S. A., Iftikhar, N., Pastar, Z. & Hosler, G. A. Keratosis Follicularis Spinulosa Decalvans Associated with Acne Keloidalis Nuchae and Tufted Hair Folliculitis. *Am. J. Clin. Dermatol.* **9**, 137–140 (2008).

85. Gloster, H. M. The surgical management of extensive cases of acne keloidalis nuchae. *Arch. Dermatol.* **136**, 1376–9 (2000).

86. Kantor, G. R., Ratz, J. L. & Wheeland, R. G. Treatment of acne keloidalis nuchae with carbon dioxide laser. *J. Am. Acad. Dermatol.* **14**, 263–7 (1986).

87. Okoye, G. A. *et al.* Improving acne keloidalis nuchae with targeted ultraviolet B treatment: A prospective, randomized, split-scalp comparison study. *Br. J. Dermatol.* **171**, 1156–1163 (2014).

88. Jumper, N., Hodgkinson, T., Paus, R. & Bayat, A. *Site-specific gene expression profiling as a novel strategy for unravelling keloid disease pathobiology*. *PLoS ONE* **12**, (2017).

89. Moon, J.-H. *et al.* Isolation and Characterization of Multipotent Human Keloid-Derived Mesenchymal-Like Stem Cells. *Stem Cells Dev.* **17**, 713–724 (2008).

90. Dietrich, C., Wallenfang, K., Oesch, F. & Wieser, R. Differences in the mechanisms of growth control in contact-inhibited and serum-deprived human fibroblasts. *Oncogene*

15, 2743–2747 (1997).

91. Liang, C.-C., Park, A. Y. & Guan, J.-L. In vitro scratch assay: a convenient and inexpensive method for analysis of cell migration in vitro. *Nat. Protoc.* **2**, 329–333 (2007).

92. Sandulache, V. C., Parekh, A., Li-Korotky, H., Dohar, J. E. & Hebda, P. A. Prostaglandin E2 inhibition of keloid fibroblast migration, contraction, and transforming growth factor (TGF)-?1?induced collagen synthesis. *Wound Repair Regen.* **15**, 122–133 (2007).

93. Fujiwara, M., Muragaki, Y. & Ooshima, A. Keloid-derived fibroblasts show increased secretion of factors involved in collagen turnover and depend on matrix metalloproteinase for migration. *Br. J. Dermatol.* **153**, 295–300 (2005).

94. Wang, H. B., Dembo, M., Hanks, S. K. & Wang, Y. Focal adhesion kinase is involved in mechanosensing during fibroblast migration. *Proc. Natl. Acad. Sci. U. S. A.* **98**, 11295–300 (2001).

95. Sonntag, K.-C. *et al.* Late-onset Alzheimer's disease is associated with inherent changes in bioenergetics profiles. *Sci. Rep.* **7**, 14038 (2017).

96. Xintaropoulou, C. *et al.* A comparative analysis of inhibitors of the glycolysis pathway in breast and ovarian cancer cell line models. *Oncotarget* **6**, 25677 (2015).

97. Divakaruni, A. S., Paradyse, A., Ferrick, D. A. & Jastroch, M. Analysis and Interpretation of Microplate-Based Oxygen Consumption and pH Data. *Methods Enzymol.* **547**, 309–354 (2014).

98. Vander Heiden, M. G., Cantley, L. C. & Thompson, C. B. Understanding the Warburg effect: the metabolic requirements of cell proliferation. *Science* **324**, 1029–33 (2009).

99. Locasale, J. W. & Cantley, L. C. Metabolic flux and the regulation of mammalian cell growth. *Cell Metab.* **14**, 443–451 (2011).

100. Liberti, M. V. & Locasale, J. W. The Warburg Effect: How Does it Benefit Cancer Cells? *Trends Biochem. Sci.* **41**, 211–218 (2016).

101. Boroughs, L. K. & DeBerardinis, R. J. Metabolic pathways promoting cancer cell survival and growth. *Nat. Cell Biol.* **17**, 351–359 (2015).

102. Lee, Y. J. *et al.* Oxidative Damage and Nuclear Factor Erythroid 2-Related Factor 2 Protein Expression in Normal Skin and Keloid Tissue. *Ann. Dermatol.* **27**, 507–16 (2015).

103. Mathew, S. *et al.* The gene for fibroblast activation protein α (FAP), a putative cell surface-bound serine protease expressed in cancer stroma and wound healing, maps to chromosome band 2q23. *Genomics* **25**, 335–337 (1995).

104. Kelly, T. Fibroblast activation protein-α and dipeptidyl peptidase IV (CD26): Cell-surface proteases that activate cell signaling and are potential targets for cancer therapy. *Drug Resist. Updat.* **8**, 51–58 (2005).

105. Rettig, W. J. *et al.* Regulation and heteromeric structure of the fibroblast activation protein in normal and transformed cells of mesenchymal and neuroectodermal origin. *Cancer Res.* **53**, 3327–35 (1993).

APPENDICES

APPENDIX A: Sample Collection

Table A1. Study participant and lesion information

Sample	Participant ID	Age of participant	Age of lesion (years)	Site	Ethnicity	Sex
Normal skin	**GSH-N-001**	32	0	left arm	Black	M
	GSH-N-005	35	0	left arm	Black	M
	GSH-N-006	30	0	left arm	Black	M
	GSH-N-008	40	0	left arm	Black	M
	GSH-N-009	30	0	left arm	Black	M
Normal scar	**GSH-NS-001**	52	40	left leg	Black	F
	GSH-NS-003	32	21	right arm	Black	M
	GSH-NS-005	73	3	stomach	Colored	F
Keloid	**GSH-KD-006-S1**	36	3	nape of neck	Black	M
	GSH-KD-006-S2		25-27	upper left arm		
	GSH-KD-007-S2	31	7	right earlobe	Black	M
	GSH-KD-008-S1	38	15	upper right arm	Black	F
	GSH-KD-008-S2		16	right earlobe		
FKN	**GSH-FKN-001**	30	6	scalp	Black	M
	GSH-FKN-002	40	3	scalp	Black	M
	GSH-FKN-004	27	8	scalp	Black	M

Table A2. Pictures of lesions and biopsy sites. Tissue culture biopsies indicated by red arrows labelled TC

Sample ID	**Sample lesion site pictures**
GSH-N-001	 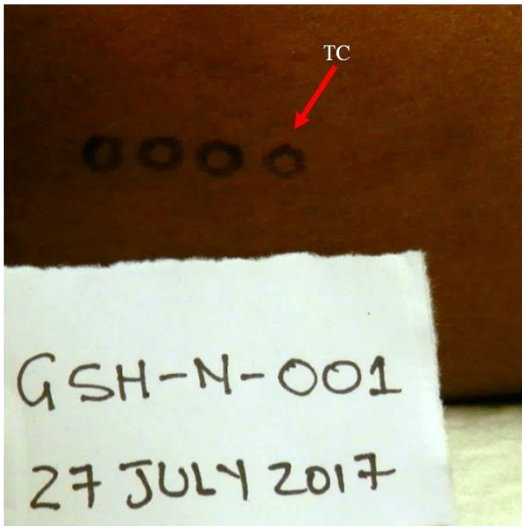

GSH-N-005	  
GSH-N-006	  

GSH-N-008	  
GSH-N-009	 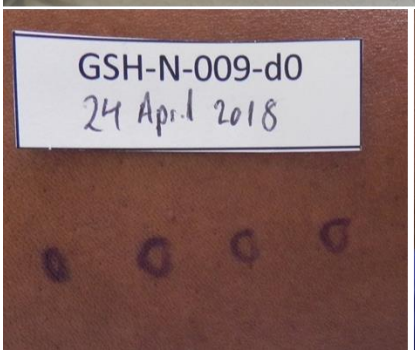 

GSH-NS-001	 
GSH-NS-003	  

GSH-NS-005	 
GSH-KD-006-S1	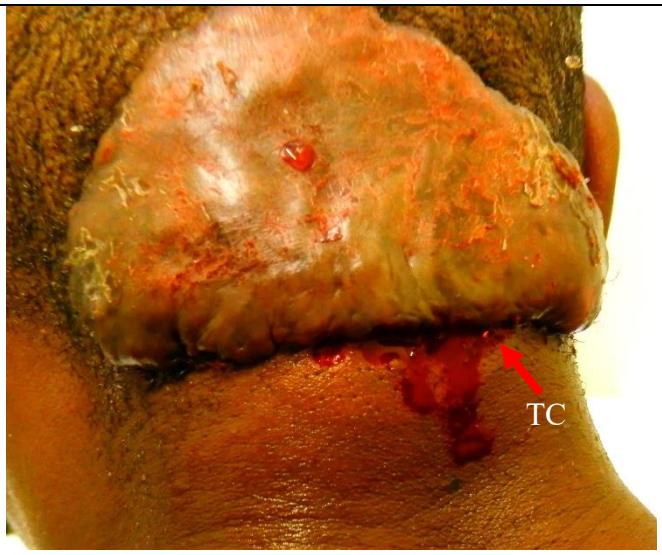

GSH-KD-006-S2	 
GSH-KD-007-S2	  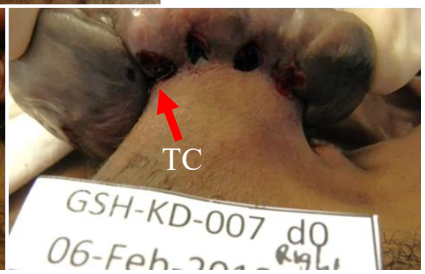

GSH-KD-008-S1	  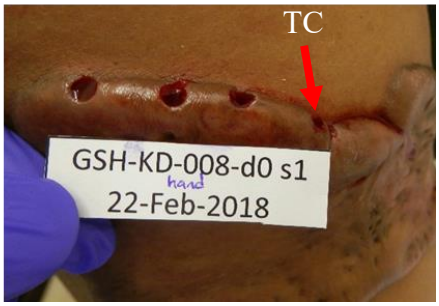
GSH-KD-008-S2	  

GSH-FKN-001	  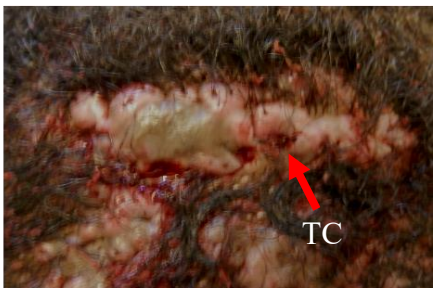
GSH-FKN-002	  

GSH-FKN-004	  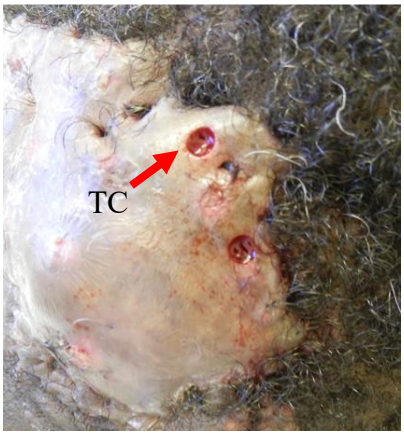

APPENDIX B: Solutions

Dulbecco's Modified Eagle's Medium (DMEM) (pH 7.4, 1L)

DMEM powder 27.06g

$NaHCO_3$ 7.4g

Autoclaved ddH_2O qs

Sterilize through a 0.2µm filter and store in aliquots at 4°C

Fetal Bovine Serum (FBS) (500ml)

FBS 500ml

Heat inactivate at 56°C (water bath) for 20 minutes

Allow to cool and store in aliquots at -20°C

Penicillin (100U/ml)/Streptomycin (100µg/ml)

Penicillin (1662U/mg) 3g

Streptomycin (750U/mg) 5g

ddH_2O 100ml

Sterilize through a 0.2µm filter and store aliquots at -20°C

Complete Fibroblast Medium (400ml) (pH 7.4)

FCS (100%) 40ml

Penicillin/streptomycin (100x) 4ml

DMEM qs

sterilize through a 0.2µm filter and store at 4°C

Trypsin/ EDTA (100ml)

Trypsin (0.05%) 0.05g

EDTA anhydrous (0.02%) 0.02g

ddH2O 100ml

sterilize through a 0.2µm filter and store at -20°C

Phosphate Buffered Saline (1xPBS) (pH 7.4) (1L)

NaCl (0.14M) 8g

Na2HPO4 (8.8M) 1.26g

KCl (2.7M) 0.2g KH2PO4 (1.47M) 0.2g ddH2O qs

Autoclave and store at 4°C

4% Paraformaldehyde (PFA) (100ml)

PFA (Merck, Germany) 4g

1xPBS qs

Heat at 50°C to dissolve and store in aliquots at -20°C

Components of RIPA complete extraction buffer

CPIC tablets (complete Protease inhibitor Tablets)

Dissolve 1 tablet in 2ml dH20 for a 25x stock

Aliquot (100µl) and store at -20oC

Pepstatin (comes as liquid)

Aliquot (100µl) and stored at -20oC

Aprotinin Powder stored at 4oC

Dissolve 1mg powder in 1m dH20

Aliquot (100µl) and store at -20oC

0.1M PMSF (phenylmethylsulfonicfluoride) Dissolve 0.087g in 5ml isopropanol

Store in a dark bottle at RT or aliquot (100µl) and store at -20oC

RIPA buffer (50ml) From each stock:

Take 1.5ml of NaCl (5M)

Add 500µl of Triton X-100 (100%)

500µl SDS (10%)

1ml Tris, pH 7.5 (1M)

Add 0.5g Deoxycholate

Add 46.5ml dH20

Filter sterilise through a 0.45 filter

Store in aliquots at 4°C

RIPA Complete Extraction Buffer (500µl) From each stock:

Take 20µl CPIC (25x)

Add 0.5µl Aproptinin (1mg/ml)

2.5µl PMSF (100mM)

0.5µl Pepstatin A

And 476µl RIPA buffer

APPENDIX C: Western Blotting

Resolving gel buffer (1.5M Tris pH 8.8, 0.4% SDS)

Weigh out: 36.342g Tris and 0.8g SDS

(Wear mask when weighing out!! Be careful)

Add it in 190ml dH20

Heat slightly to dissolve (+/- 190ml)

Add drops of concentrated HCL to pH

Then make up to 200ml final volume

Store at 4°C

Stacking gel buffer (0.5M Tris pH 6.8, 0.4% SDS)

Weigh out: 6.057g tris

Add 0.4g SDS (wear mask when weighing out)

Add 90ml of ddH_2O

10x Running buffer (0.25M Tris, 1.92M Glycine, 1% SDS)

Weigh out: 30.2g Tris and 144g Glycine

10g SDS (wear mask when weighing out)

Make up to 1L with ddH_2O

1x Running buffer (0.025M Tris, 0.192M Glycine, 0.01%SDS)

Take 100ml of 10x running buffer

Add 900ml of ddH20

10x Transfer buffer (0.31M Tris, 1.92M Glycine)

Weigh out: 144g glycine and 38g of Tris

Make up to 1L with ddH_2O

Store at 4°C

1x Transfer buffer (0.031M Tris, 0.192M Glycine)

Take 100ml of 10x Transfer buffer 81

Add to it 700ml ddH_2O

Then, add methanol/isopropanol (methanol can be technical grade)

10x Tris Buffered Saline (TBS) pH 7.5

Weigh out: 60.5g Tris and 87.6g NaCl

Dissolve in 700ml of dd H_2O

Then pH to 7.5

Make up to 1L

1x TBS-Tween

Take 100ml of 10x TBS pH 7.5

Add 900ml of ddH_2O

Add 1ml Tween20

5x Loading Buffer (LB)

Weigh out 1.75g Tris 82

Add 30ml of glycerine

Make it up to 40ml with ddH20

pH it to 6.8 with 1N HCL

Add 5g SDS/SLS

Make up to 50ml

5x Loading dye

Heat up 5x loading buffer to allow SDS precipitate to dissolve

Mix with 100µl 5x loading buffer (2 parts)

50µl β-mercaptoethanol (1 part)

50µl 0.025% bromophenol blue (1 part)

Use at 1x loading dye on the gel.

Ponceau S stain (0.1% (w/v) ponceau S in 5% (v/v) acetic acid)

Weigh 1g Ponceau S

Add 50ml acetic acid

Make up to 1L with ddH20

Store at 4°C. Do not freeze

A

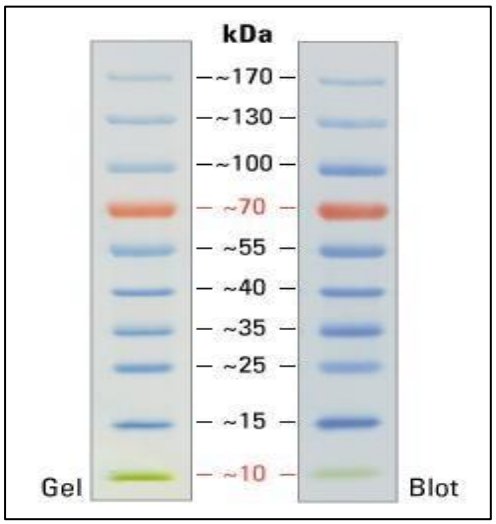

B

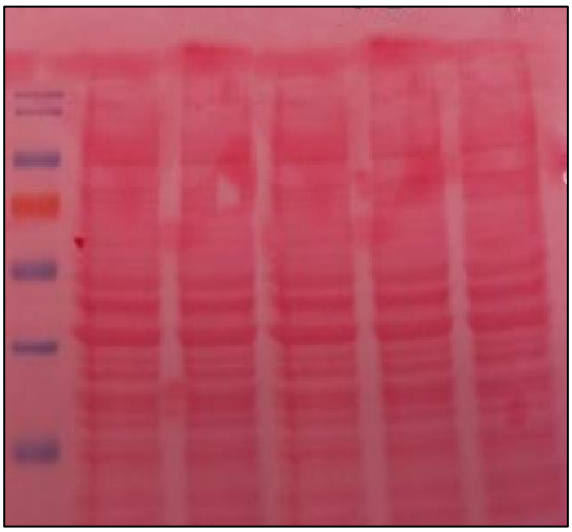

Figure A. Western blot membrane post electrophoresis and stain. A) PageRuler Prestained Protein Marker; B) Stained membrane on right side

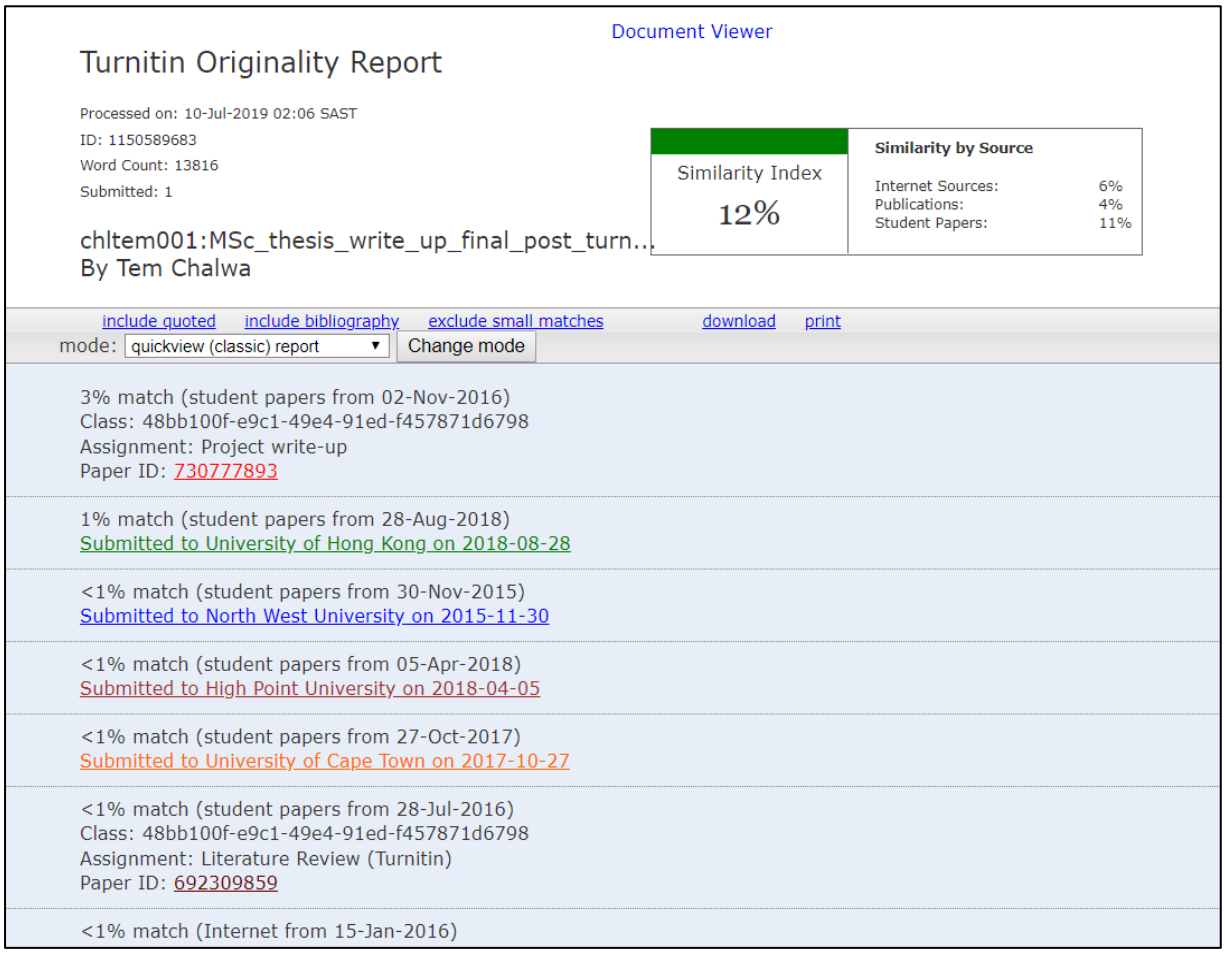

Document Viewer

Turnitin Originality Report

Processed on: 10-Jul-2019 02:06 SAST
ID: 1150589683
Word Count: 13816
Submitted: 1

chltem001:MSc_thesis_write_up_final_post_turn...
By Tem Chalwa

Similarity Index
12%

Similarity by Source

Internet Sources:	6%
Publications:	4%
Student Papers:	11%

include quoted include bibliography exclude small matches download print

mode: quickview (classic) report Change mode

3% match (student papers from 02-Nov-2016)
Class: 48bb100f-e9c1-49e4-91ed-f457871d6798
Assignment: Project write-up
Paper ID: 730777893

1% match (student papers from 28-Aug-2018)
Submitted to University of Hong Kong on 2018-08-28

<1% match (student papers from 30-Nov-2015)
Submitted to North West University on 2015-11-30

<1% match (student papers from 05-Apr-2018)
Submitted to High Point University on 2018-04-05

<1% match (student papers from 27-Oct-2017)
Submitted to University of Cape Town on 2017-10-27

<1% match (student papers from 28-Jul-2016)
Class: 48bb100f-e9c1-49e4-91ed-f457871d6798
Assignment: Literature Review (Turnitin)
Paper ID: 692309859

<1% match (Internet from 15-Jan-2016)

This thesis/dissertation has been submitted to the Turnitin module (or equivalent similarity and originality checking software) and I confirm that my supervisor has seen my report and any concerns revealed by such have been resolved with my supervisor